Copper(II)-Immobilized Covalent Organic Framework as Efficient and Recyclable Catalyst for the Sustainable Synthesis of Imidazo[1,2-a]pyridines

Dissertation submitted to
Visvesvaraya National Institute of Technology, Nagpur
In partial fulfilment of the requirements for the award of the degree

Master of Science

In

Chemistry

by

Naresh Bahalia (MS23CHM009)

under the guidance of

Dr. Umesh R. Pratap

Department of Chemistry
Visvesvaraya National Institute of Technology
Nagpur 440010 (India)

May 2025

Copper(II)-Immobilized Covalent Organic Frameworks as Efficient and Recyclable Catalysts for the Sustainable Synthesis of Imidazo[1,2-a]pyridines

Dissertation submitted to
Visvesvaraya National Institute of Technology, Nagpur
In partial fulfilment of the requirements for the award of the degree

Master of Science

In

Chemistry

by

Naresh Bahalia (MS23CHM009)

under the guidance of

Dr. Umesh R. Pratap

Department of Chemistry

Visvesvaraya National Institute of Technology

Nagpur 440010 (India)

May 2025

©Visvesvaraya National Institute of Technology (VNIT) 2009

Department of Chemistry
Visvesvaraya National Institute of Technology, Nagpur

Declaration

I, Naresh Bahalia hereby declare that this dissertation titled **"Copper(II)-Immobilized Covalent Organic Frameworks as Efficient and Recyclable Catalysts for the Sustainable Synthesis of Imidazo[1,2-a]pyridines"** is carried out by me in the Department of Chemistry of Visvesvaraya National Institute of Technology, Nagpur. The work is original and has not been submitted earlier whole or in part for the award of any degree/diploma at this or any other Institution / University.

Naresh Bahalia(MS23CHM009)
Date:

Certificate

This is to certify that the dissertation titled **"Copper(II)-Immobilized Covalent Organic Frameworks as Efficient and Recyclable Catalysts for the Sustainable Synthesis of Imidazo[1,2-a]pyridines"** is submitted by **Naresh Bahalia** in partial fulfilment of the requirements for the award of the degree of **Master of Science in Chemistry, VNIT Nagpur.** The work is comprehensive, complete and fit for final evaluation.

Dr. Umesh R. Pratap
Associate Professor
Department of Chemistry, VNIT Nagpur

Head, Department of Chemistry
VNIT, Nagpur
Date: 13/05/2025

Visvesvaraya National Institute of Technology, Nagpur

Department of Chemistry

Non-Plagiarism Certificate

Certified that M.Sc. dissertation titled **"Copper(II)-Immobilized Covalent Organic Frameworks as Efficient and Recyclable Catalysts for the Sustainable Synthesis of Imidazo[1,2-a]pyridines"** submitted by **Naresh Bahalia** Enrolment No. **MS23CHM009** ID No. 30419 has been checked for plagiarism using TURNITIN software, and the overlap is found within prescribed limits. A summary of the report is given below.

ORIGINALITY REPORT

17%	11%	14%	%
SIMILARITY INDEX	INTERNET SOURCES	PUBLICATIONS	STUDENT PAPERS

PRIMARY SOURCES

Dr. Umesh R. Pratap
Associate Professor
Department of Chemistry
Visvesvaraya National Institute of Technology Nagpur

Naresh Bahalia
MS23CHM009
ID-30419

Acknowledgment

I would like to express my sincere gratitude to my supervisor, **Dr. Umesh R. Pratap**, for his exceptional guidance, unwavering support, and invaluable mentorship throughout my journey as a M.Sc. student. I am forever indebted for his remarkable expertise, patience, and dedication in guiding me through conducting research and writing this thesis. Your astute insights, constructive feedback, and visionary guidance have been instrumental in shaping the direction of my work. You have consistently challenged me to think critically, encouraged me to explore new avenues of inquiry, and inspired me to reach for excellence.

I would also like to express my gratitude to my Ph.D. scholars, Mr. Ankit Verma, Ms. Shivani Bhagat, Ms. Sneha Wahurwagh and Mr. Pankaj Kumar Gautam, who have accompanied me on this academic journey. Your camaraderie, intellectual discussions, and collaborative efforts have enriched my experience in countless ways. Through our shared challenges and triumphs, I have not only grown as a researcher but also formed lasting friendships and a supportive network. Your diverse perspectives, stimulating debates, and willingness to lend a helping hand have been invaluable, and I am grateful for the opportunity to be part of such an inspiring community.

Furthermore, I would like to express my heartfelt gratitude to my lab mate, Mr. Pranjal Singh, and all those who generously offered their help and support throughout this journey. A special note of thanks goes to my beloved Mom, Dad, and my Brother, whose unwavering love, encouragement, and inspiration have been the cornerstone of my strength and perseverance.

Naresh Bahalia

Abstract:

Covalent Organic Frameworks (COFs) are a versatile class of crystalline polymers with tunable architectures, capable of coordinating with metal ions and nanoparticles to generate highly effective heterogeneous catalysts. In this study, we present the synthesis of a functionalized hydrazone-linked Covalent Organic Framework (CTN-COF). The hydrazone linkages within the framework serve as strategic anchoring sites for the immobilization of Cu(II), facilitating the straightforward, one-step formation of Cu(II)@CTN-COF. This unique feature makes the COF highly effective for metal ion loading and contributes to its catalytic stability. The successful formation of the Cu(II)@CTN-COF was confirmed by PXRD (crystallinity), IR (functional groups), Solid State NMR (structural analysis), FE-SEM and HR-TEM (morphology), BET (surface area and porosity), and XPS (elemental composition and oxidation state). Cu(II)@CTN-COF demonstrated remarkable catalytic efficiency in a multicomponent cascade reaction involving the A^3-coupling of heterocyclic amidines with aldehydes and alkynes, followed by 5-exo-dig cycloisomerization and a prototropic shift. This one-pot transformation enabled the sustainable and high-yielding synthesis of biologically relevant, N-fused imidazole derivatives. Importantly, the catalyst exhibited excellent recyclability, maintaining high performance over multiple reaction cycles. This work underscores the potential of COFs as robust platforms for the development of heterogeneous catalysts tailored for complex organic transformations such as A^3-coupling reactions.

LIST OF CONTENTS

CHAPTER-1

1. Introduction 2

1.1 Covalent Organic Frameworks 2

1.2 Structure of Covalent Organic Frameworks 3

1.2.1 Dimensionality and Network Design 3

1.2.2 Building blocks and Bonding motifs 4

1.2.3 Pore structures and Surface Properties 4

1.2.4 Crystallinity and Structural Integrity 4

1.3 Classification and Linkages of COFs 5

1.3.1 2D Covalent Organic Frameworks 5

1.3.2 3D Covalent Organic Frameworks 6

1.3.3 Linkages in Covalent Organic Frameworks 6

1.4 Synthetic Methods of Preparation of COFs 6

1.4.1 Solvothermal Synthesis 6

1.4.2 Ionothermal Synthesis 7

1.4.3 Microwave assisted Synthesis 8

1.4.4 Mechanochemical Synthesis 9

1.4.5 Sonochemical Synthesis 9

1.5 Post-Synthetic Modifications 10

1.5.1 Post-synthetic modification of COFs by Metalation 11

1.5.2 Post-synthetic modification through Functionalization 12

1.6 Applications of Covalent Organic Frameworks 13

1.6.1 COF in CO_2 Capture 13

1.6.2 COF as Photocatalyst 14

1.6.3 COF as a Heterogeneous Catalyst in Organic Synthesis 15

CHAPTER-2

2. Synthesis of Cu(II) functionalized Hydrazone based CTN COF

2.1 Hydrazone-based COF 18

2.2 Experimental Section 19

2.2.1 Materials and Methods 19

2.2.2 Synthesis of BTH & TTTB (Linkers) 19

2.2.3 Synthesis of CTN COF 20

2.2.4 Post-Synthetic Incorporation of Cu(II) into CTN COF 21

2.3 Characterization of CTN COF and Cu(II)@CTN COF 21

2.3.1 FT-IR Analysis 22

2.3.2 P-XRD Analysis 23

2.3.3 Thermogravimetric Analysis 25

2.3.4 Brunauer-Emmett-Teller (BET) surface area analysis 26

2.3.5 Field Emission Scanning Electron Microscope (FE-SEM)
Analysis of CTN COF 27

2.3.6 Field Emission Scanning Electron Microscope (SEM)
Analysis of Cu(II)-CTN COF 28

2.3.7 EDS Analysis and Elemental Mapping 29

2.3.8 X-ray photoelectron spectroscopy (XPS) 31

CHAPTER-3

3.Catalytic application of Cu(II)-CTN COF 33

3.1 Introduction about Imidazo[1,2-a]pyridines 34

3.2 Result and Discussion 37

3.3 Plausible Mechanism of the reaction 42

3.4 Experimental Section 42

3.4.1 Materials and Equipment 42

3.4.2 General synthetic procedure for the one-pot synthesis of imidazo[1,2-a]pyridine derivatives. 43

3.4.3 Spectral data of 4-(3-benzylimidazo[1,2-a]pyridin-2-yl)benzonitrile 43

3.4.4 Spectral data of 3-benzyl-2-(3-nitrophenyl)imidazo[1,2-a]pyridine 43

3.5 Recyclability of Catalyst 46

3.6 Conclusion 47

S.N	Title of Figures	Pg.No.
1	Diverse applications of Covalent Organic Frameworks (COFs)	3
2	Symmetry directed design of COF Topologies based on Monomer geometry	5
3	Solvothermal Synthesis of COF	7
4	Ionothermal Synthesis of CTF-2	8
5	Microwave assisted synthesis of COF-1	9
6	Overview of Post-Synthetic Modification Strategies for Covalent Organic Frameworks	10
7	Incorporation of Pd(II) into COF-LZU1	11
8	Functionalization of imine-based COF into stable aromatic framework	12
9	Characteristic properties and various applications of COF	13
10	Functionalization of COF-300 for the adsorption of CO_2	14
11	Photocatalytic activity of Covalent Organic Framework[1]	15
12	Catalytic activity of COF and metal incorporated COF	16
13	Comparative FT-IR analysis of a) TTTB, b) BTH, c) CTN COF, d) Cu(II)@CTN COF	22
14	Comparative P-XRD analysis of a)TTTB, b) BTH, c) CTN COF, d) Cu(II)@CTN COF.	23
15	Low angle P-XRD Analysis of CTN COF	24
16	Thermogravimetric Analysis of CTN COF and Cu(II)@CTN COF16 BET isotherms of a) CTN COF b) Cu(II)@ CTN COF	25
17	BET isotherms of a) CTN COF b) Cu(II)@ CTN COF	26
18	FE- SEM Images of CTN COF	27
19	18 FE- SEM Images of Cu(II)@CTN COF	28
20	Particle distribution curve of Cu(II)@CTN COF	29
21	EDS and Elemental analysis of CTN COF	30
22	EDS and Elemental analysis of Cu(II)@CTN COF	30

23	XPS Analysis of Cu(II)@CTN COF . a) High resolution full XPS survey, b) C1s Spectra, c) N1s Spectra, d) O1s Spectra	**31**
24	High resolution Full XPS survey of Cu 2p	**32**
25	Potent biological activity of Imidazo[1,2-a]pyridines	**34**
26	Comparative FT-IR of fresh and used Catalyst	**46**

CHAPTER-1

Introduction to Covalent Organic Framework

1.1 Covalent Organic Frameworks

Covalent Organic Frameworks(COFs) are porous crystalline materials constructed through strong covalent bonds in a periodic arrangement of organic building blocks. Their unique combination of low density, high thermal and chemical stability, and permanent porosity has attracted significant research interest. These features have led to various applications, including gas storage, catalysis, optoelectronics, environmental remediation, and drug delivery[2], [3].

Covalent bonds are fundamental to the stability and strength of COFs, as they provide the backbone of their extended network structures. In nature, covalent bonds are solids such as diamond, silicon carbide, and boron nitride that exhibit exceptional mechanical and thermal properties. Organic chemistry initially mastered covalent bond formation in zero-dimensional molecules, while polymer chemistry extended this to dimensional chains. However, creating ordered two- and three-dimensional covalent structures remained an obstacle until 2005 when Yaghi and co-workers pioneered the synthesis of COFs using dynamic covalent chemistry[4], [5]. Unlike branched polymers, COFs require in situ Crystallization due to their insolubility and high bond energies, making their synthesis more complex.

During the synthesis of covalent networks, multiple structural variations with different free energies can emerge. Without controlled reversibility, kinetic trapped amorphous products tend to dominate. To overcome this reversible bond formation strategies are employed to allow self-correction and error repairing during crystallization[4].

However, since covalent bonds typically require high activation energy to undergo reversible formation, conventional thermal methods are often ineffective under mild conditions. Building on this success, various reversible condensation reactions, such as Schiff base reactions, boronate ester formations, Spiro borane condensation, and imide condensation have been explored for COF synthesis[6], [7], [8], [9]. Guided by the principle of reticular chemistry, both two-dimensional and three-dimensional COFs have been designed with tailored functionality.

With continuous advancements in synthesis techniques and functionalization strategies, COFs have emerged as a powerful class of materials in solid-state chemistry. Their pre-designable structure, combined with their exceptional stability and porosity, open new possibilities for next-generation materials in energy storage, Sensing, and separation science[10], [11].

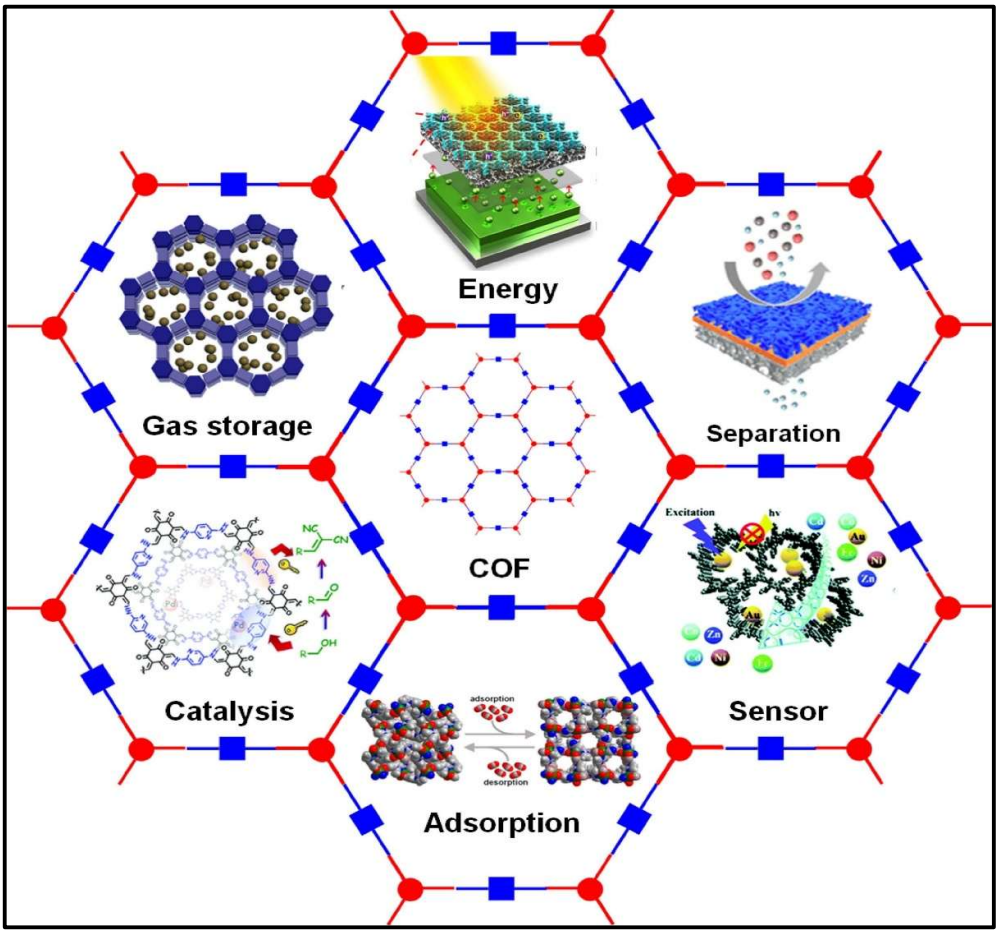

Fig. 1 Diverse applications of Covalent Organic Frameworks (COFs)[12]**.**

1.2 Structure of Covalent Organic Framework

The structural organization of COFs results in highly ordered frameworks with tuneable porosity, making them attractive for applications such as catalysis, gas storage, and separation technologies. Different structural aspects of these porous organic materials have been further discussed as follows.

1.2.1 Dimensionality and Network Design

COFs are categorized into two primary structural types: two-dimensional (2D) and three-dimensional (3D) frameworks. In 2D COFs, the organic units are covalently connected in planar layers that stack through non-covalent interactions such as π-π stacking. This layered arrangement creates uniform, column-like channels, enhancing their surface area and facilitating diffusion. On the other hand, 3D COFs feature extended covalent bonding in all directions, forming rigid, interwoven networks[13].

1.2.2 Building blocks and Bonding motifs

The assembly of COFs is based on the selection of organic precursors that determine the final framework's stability and functionality. Key structural components include organic linkers and functional nodes connected through covalent bonds such as boronate esters, imine, hydrazone, and amide linkages. The type of covalent bond formation dramatically influences the stability and reactivity of COFs. For example, imine-based COFs exhibit excellent chemical and thermal stability, while boronate ester linkages are known for their high crystallinity and well-defined porosity but may be sensitive to moisture[13].

1.2.3 Pore Structures and Surface Properties

One of the defining characteristics of COFs is their intrinsic porosity, which results from the precise arrangement of monomers within the framework. The pore size and shape can be tailored by modifying the structures of the organic building units, enabling selective molecular interactions. These materials possess high surface areas making them suitable for various adsorption-based applications. Their tunable pore size also allows for site-selective separation and catalysis[14].

1.2.4 Crystallinity and Structural Integrity

Unlike conventional porous organic materials, COFs possess a high degree of crystallinity due to the reversible nature of their covalent bond formations. This reversibility allows self-correction during synthesis during synthesis, leading well well-ordered structures. However long-term stability of COFs depends on the strength of their covalent linkages. For example, amide and imine-linked COFs show excellent resistance to hydrolysis, whereas boronate ester-based frameworks are more susceptible to degradation in humid conditions. Enhancing the stability of COFs is a key focus in research, particularly for their application in real-world conditions[15].

1.3 Classifications and Linkages in COFs

Covalent Organic Frameworks are crystalline, porous polymers formed through the covalent bonding of monomers. They are broadly classified into two main types based on their structural dimensionality: 2D and 3D COFs. This classification depends on the geometry of the building blocks and the directionality of their linkage. While 2D COFs form layered sheet-like structures, 3D COFs exhibit extended frameworks in all three spatial dimensions.

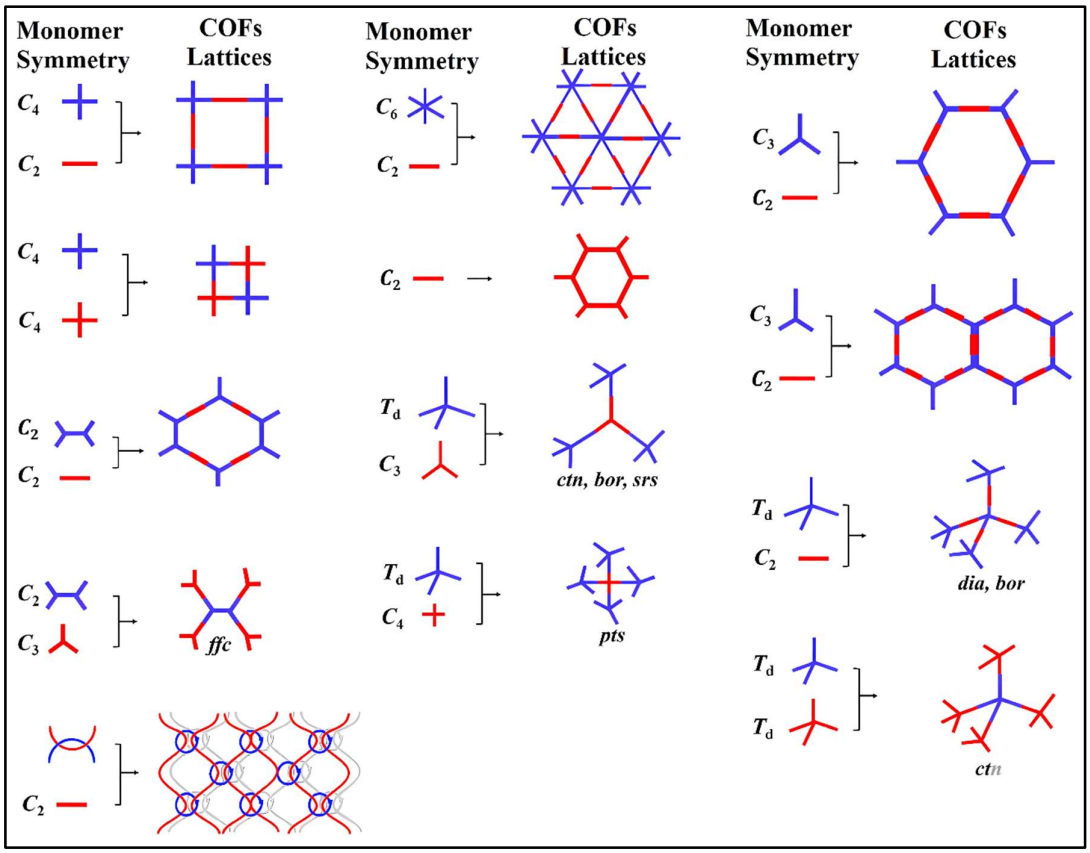

Fig.2 Symmetry directed design of COF Topologies based on Monomer geometry[16]

a. 2D Covalent Organic Frameworks

Two-dimensional covalent organic frameworks are constructed by linking planar organic building blocks through covalent bonds, resulting in layered structures that extend in two dimensions. These layers stack on top of each other via pi-pi stacking, Van der Waals forces, or hydrogen bonding, forming highly ordered crystalline frameworks. The in-plane periodicity of 2D COFs typically gives rise to well-defined pore geometries, such as

hexagonal, square, or rectangular arrangements, with high surface areas and tunable pore sizes. Due to their directional structures and pi-conjugated backbones,2D COFs have various applications including sensing, organic electronics, energy storage, and photocatalysis.

b. 3D Covalent Organic Frameworks

Three-dimensional covalent organic frameworks are built using multidirectional building blocks, such as tetrahedral, trigonal pyramidal, or other nonplanar monomers, which allow the network to extend in all three spatial dimensions. Unlike 2D COFs which form layered structures, 3D COFs possess interconnected, rigid frameworks with defined topologies such as diamond(dia), pts, and nets. The synthesis of 3D COFs is generally more complex due to challenges in achieving long-range order and crystallinity; however, they offer significant advantages in terms of structural rigidity, higher pore accessibility, and isotropic properties. Applications are quite similar to 2D COFs[16]

c. Linkages in Covalent Organic Frameworks

The structural stability and overall functionality of Covalent Organic Frameworks(COFs) are strongly influenced by the type of covalent linkages connecting their organic building units.

Linkages are typically formed via dynamic covalent chemistry, which enables self-correction during the synthesis process and contributes to the high crystallinity of the final frameworks. Commonly used linkages include boronic ester, imine hydrazone, azine, triazine, amide, and ketoenamine, each offering unique levels of chemical robustness and functionality versatility[4], [15], [17]. Additionally, the formation of these linkages highly depends on the reaction environment and synthetic conditions. A thorough understanding of linkage chemistry is essential for designing COFs with properties tailored to their intended functional roles.

Here are some examples of linkages that are commonly found in COFs

1.4 Synthetic Methods of Covalent Organic Frameworks

The synthesis of Covalent Organic Frameworks (COFs) involves the formation of extended crystalline networks through the covalent linking of organic building blocks.

Several synthetic methods have been developed to construct COFs with varying degrees of crystallinity, porosity, and functionalization[18]. The major methods includes:

1.4.1 Solvothermal Synthesis

Solvothermal synthesis is one of the most widely use and historically significant methods for the preparation of Covalent Organic frameworks. First reported in 2005 by Yaghi and co-workers during the synthesis of COF-1 and COF-5, this method involves the reaction of organic monomers in a sealed vessel(generally autoclave) under elevated temperature(120-160ºC) and pressure using a suitable solvent system[19]. The solvothermal route has since become a standard approach due to its ability to produce highly crystalline, porous COF structure.

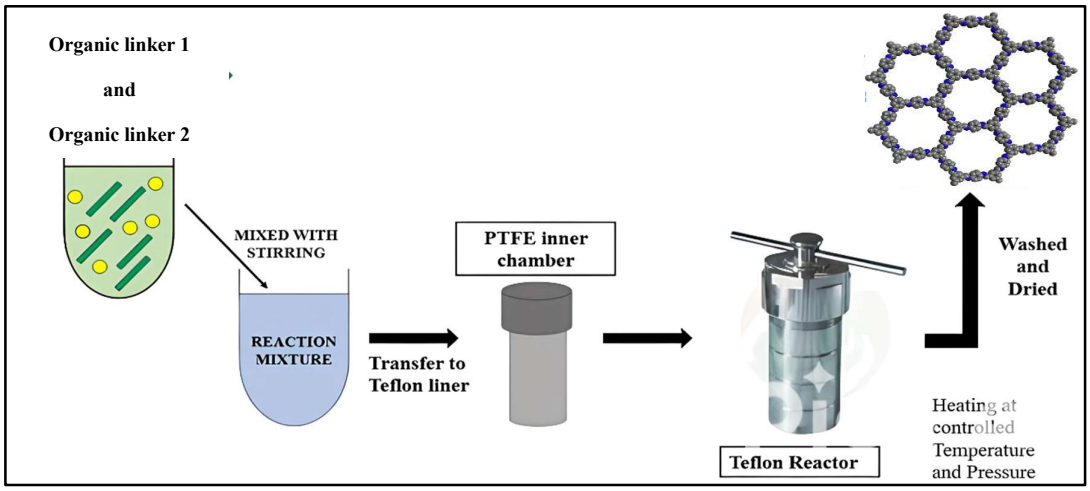

Fig. 3 Solvothermal Synthesis of COF

In this method, reversible covalent bond formation, such as a boronate ester, imine, or triazine linkage, is key to the error correction process during framework formation, allowing the gradual assembly of long-range ordered structures. However, the method is relatively time-consuming and may involve harsh conditions or solvents, creating scalability and sustainability issues[2]. Furthermore, solvothermal synthesis continues to serve as a benchmark for evaluating alternative methods such as microwave, mechanochemical, and sonochemical approaches.

1.4.2 Ionothermal synthesis

Ionothermal synthesis is a technique in which solid materials are generated in the presence of ionic liquid or molten salt, which functions as both a solvent and a catalytic medium. This process is typically carried out at elevated temperatures, often around 400°C, and under high-pressure conditions within a sealed, thick-walled reaction vessel such as a Pyrex tube or quartz ampoule[14].

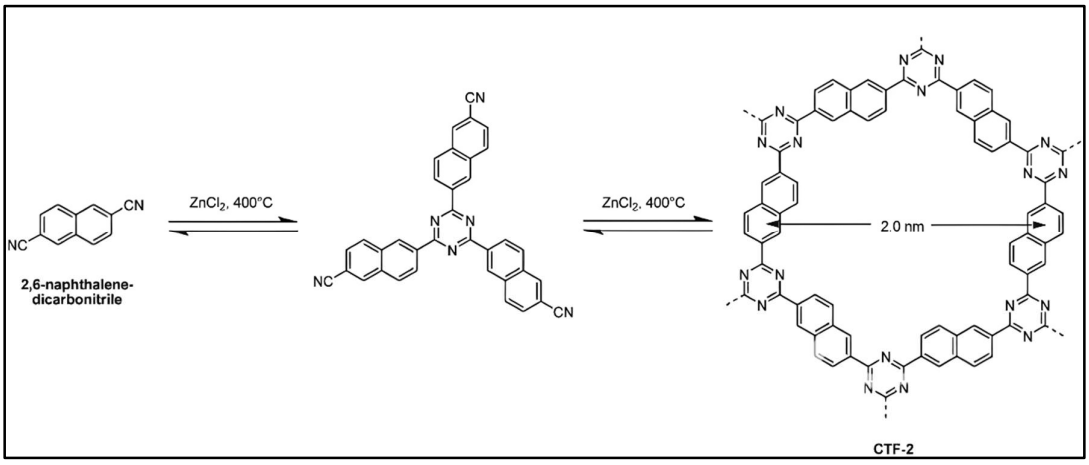

Fig. 4 Ionothermal Synthesis of CTF-2 [20]

The use of ionic liquid offers unique advantages, involving solubility of precursors and controlled reaction kinetics, making it a valuable approach for the synthesis of highly stable frameworks. For example, Bojdys et al. synthesized CTF-2, which was obtained by the heating of 2,6-napthalenedicarbonitrile in the presence of ZnCl2 within a sealed quartz glass ampoule at 400°C for 40 hr. via an ionothermal condensation process. Additionally, the resulting CTFs often exhibit an amorphous nature with a lack of long-range molecular order, which can compromise their crystallinity and structural integrity. These factors have contributed to the relatively limited adoption of the ionothermal method for COF and CTF synthesis.

1.4.2 Microwave Assisted Synthesis

Microwave irradiation has gained significant attention as an efficient and rapid method for the synthesis of covalent Organic Frameworks (COFs). Compared to traditional solvothermal techniques, MW-assisted synthesis offers several advantages, including reduced reaction times, improved crystallinity, enhanced purity, and better control over reaction parameters[21]. MW heating enables rapid and uniform energy transfer, drastically reducing reaction time. For example, COF-5 and COF-102 have been

synthesized in just 20 minutes at 100 °C, which is 200 times faster than the conventional solvothermal approach[22]. Its scalability has also been demonstrated, making MW-

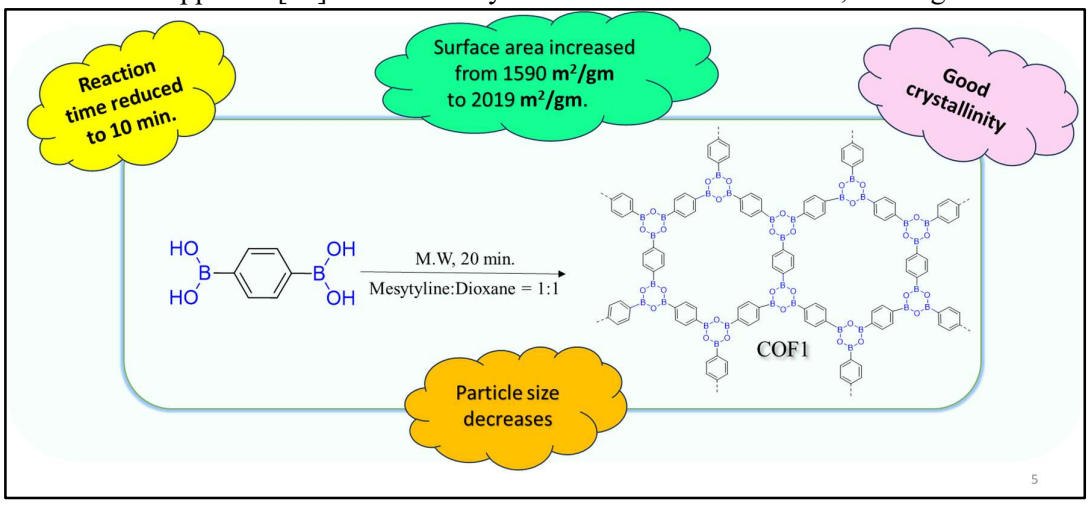

Fig. 5 Microwave assisted synthesis of COF-1 [23]

assisted synthesis a promising approach for large-scale COF production. With its numerous advantages, microwave-assisted COF synthesis is paving the way for the development of novel functional materials with advanced properties.

1.4.3 Mechanochemical Synthesis

Mechanochemical synthesis is a solvent-free and sustainable approach for preparing Covalent Organic Frameworks. It utilizes mechanical forces such as grinding, ball milling, or extrusion to induce chemical reactions. This method eliminates toxic solvents, reduces reaction times, and enhances sustainability while maintaining high crystallinity and porosity. Mechanochemically synthesized COFs have demonstrated great potential in applications such as gas storage, separation, heterogeneous catalysis, and energy storage due to their high surface area, stability, and tunability[24]. With its efficiency, scalability, and environmental benefits, mechanochemical synthesis continues to be a promising approach for the green and rapid production of COFs.

1.4.4 Sonochemical Synthesis of COFs

Sonochemical synthesis is an efficient and environmentally friendly approach for preparing Covalent Organic Frameworks, employing high-frequency ultrasonic waves to drive chemical reactions. The process relies on acoustic activation, the rapid formation and collapse of microscopic bubbles, which creates localized hotspots with extremely high temperatures and pressures for short durations[25]. These conditions accelerate reaction

rates and enhance mixing, enabling fast and uniform COF formation under mild conditions. This method often produces COFs with good crystallinity and fewer impurities, while also reducing the need for high temperatures, long reaction times, and toxic solvents. The technique is scalable, energy-efficient and compatible with green chemistry principles, making it a valuable strategy for rapid and sustainable COF synthesis

1.5 Post-Synthetic Modifications of Covalent Organic Frameworks

Post-synthetic modification (PSM) refers to the chemical transformation of COFs after their initial construction, allowing the incorporation of new functional groups or fine-tuning of properties without disturbing the overall framework integrity. Since COFs are assembled through reversible covalent bonds and feature well-defined, accessible pores, they offer an ideal platform for PSM strategies[26].

Fig.6 Overview of Post-Synthetic Modification Strategies for Covalent Organic Frameworks[26]

Why PSM ?

- Enhancing functionality: Introduce active sites for catalysis, sensing, or adsorption[27].
- Tailoring properties: Modify pore environment to improve selectivity, stability, or solubility[28].
- Expanding application scope: Enable COFs to participate in diverse applications, such as drug delivery, separation, and energy storage[28].

The following are some methods through which PSM is generally done.

1.5.1 Post-Synthetic Modification Through Metalation

Introducing metal ions into COFs through post synthetic modification is a powerful strategy to create advance materials with enhanced catalytic properties. The well-defined porosity and regular distribution of binding sites in COFs provide an ideal scaffold for uniform metal incorporation, enabling control over active site positioning and catalytic behaviour[4]. Imine and Hydrazone linked COFs are particularly attractive for metalation, as the lone pair of electrons on the nitrogen atom offers strong coordination with transition metals. Various metal ions have been introduced into COFs using this approach for e.g. Pd^{2+}, Cu^{2+}, Ni^{2+}, Co^{2+}, $Fe^{2+/3+}$ have been incorporated.

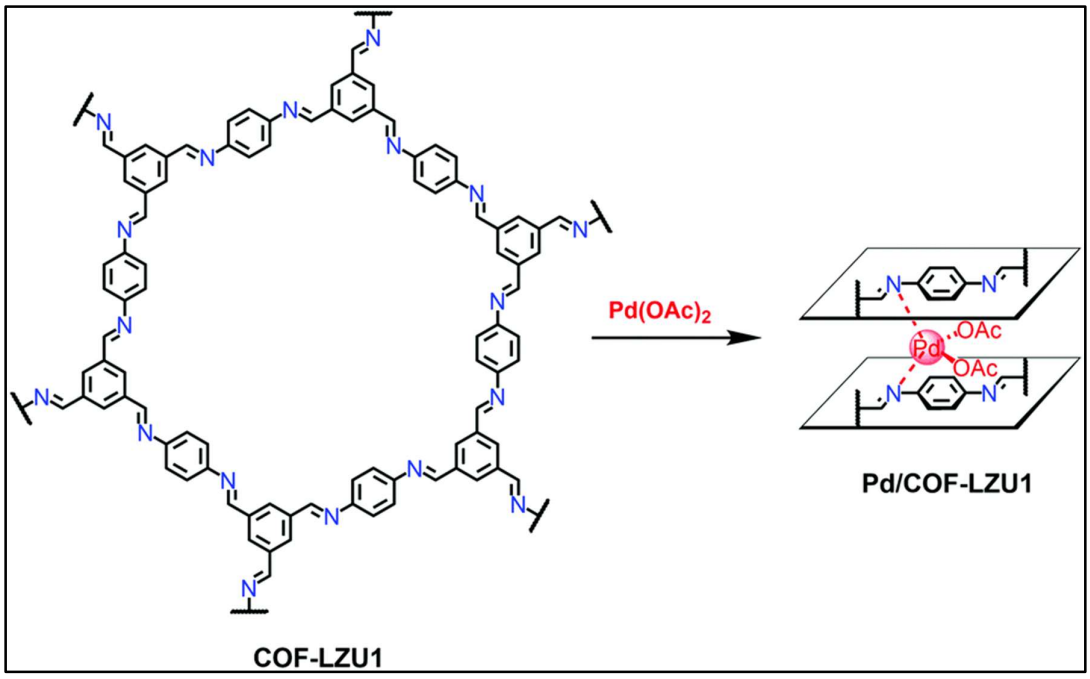

Fig. 7 Incorporation of Pd(II) into COF-LZU1[29]

A prominent demonstration of post synthetic metalation in COFs involves the integration of palladium ions into Imine based COF-LZU1[30]. This COF features a two-dimensional eclipsed layer structure with well aligned nitrogen atoms that serve as coordination sites for metal ions, and then it was further used for catalytic applications. The process retained crystallinity of the COF and allowed efficient metal coordination, as confirmed b as confirmed by XPS, which revealed a shift in biding energy due to electron donation from the imine nitrogen atoms to the Pd(II).Metalated COFs exhibit excellent chemical and thermal stability, often operating efficiently under mild, green conditions. Their robustness and recyclability make them attractive for different applications such as Catalyst for Organic Transformations, Electrocatalyst[31], Chemical Sensing and light harvesting[1].

1.5.2 Post-Synthetic Modifications through Functionalization

Post-synthetic modification through functionalization offers a strategic solution into a key challenge in the development of Covalent Organic Frameworks. Balancing the reversibility required for crystallinity with the stability necessary for practical applications. Reversible linkages, such as imine bonds, are ideal during COF formation due to their ability to self heal defects, thus promoting long-range order. This post-synthetic strategy effectively circumvents the uncertainties of direct synthesis, allowing access to robust, highly ordered COFs suitable for demanding environments. As a result, linkage transformation has emerged as a powerful tool for tailoring COF properties and expanding their functional landscape. For example, Lotsch and his team used a post-synthetic "locking" approach to convert a 2D imine-linked COF into a more stable thiazole-linked version. Liu and colleagues enhanced the stability of imine-linked COFs by transforming them into stable aromatic frameworks through an aza-Diels–Alder cycloaddition reaction[2], [32].

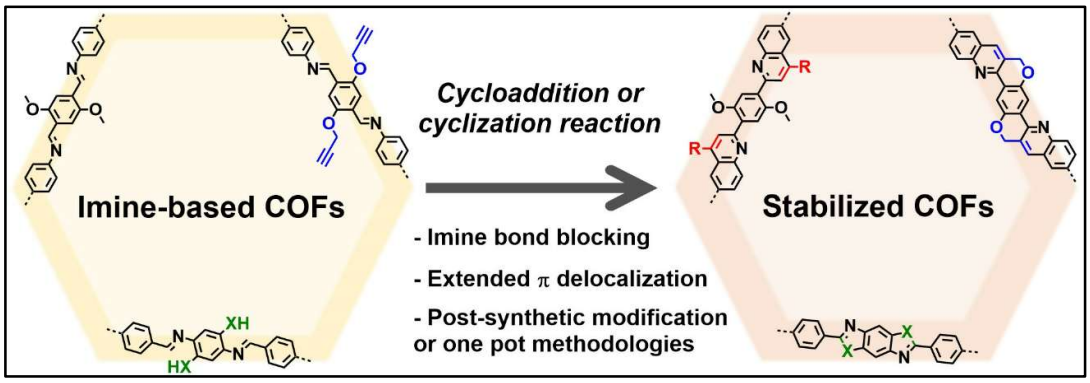

Fig. 8 Functionalization of imine based COF into stable aromatic framework[32] **.**

Including these two post synthetic modifications, there are some other post synthetic modifications available like –

1.6 Applications of Covalent Organic Frameworks

In this context, COF refers to Covalent Organic Framework, a type of crystalline, porous material composed of organic molecules connected through robust covalent bonds. Their extensive range of applications stems from features like large surface area, adjustable pore sizes, and excellent chemical stability.

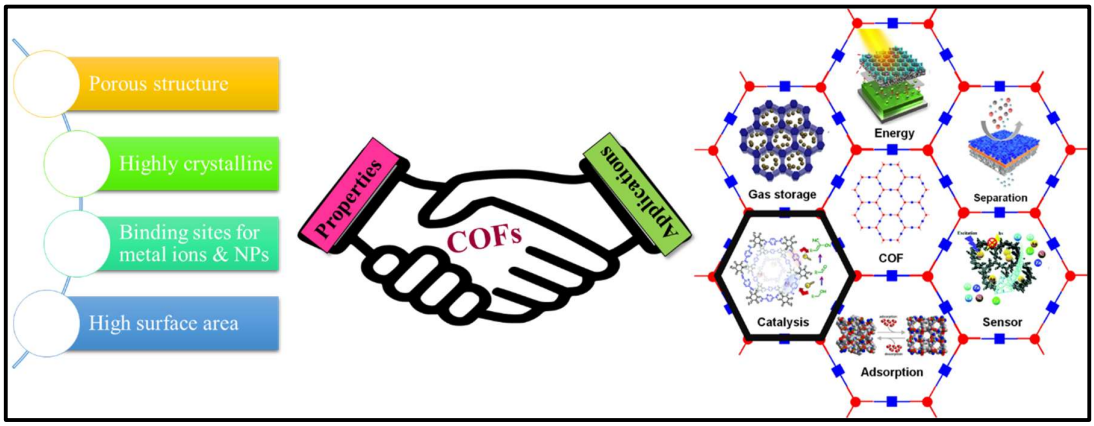

Fig. 9 Characteristic properties and various applications of COF

1.6.1 COF in CO2 Capture Process

Covalent Organic Frameworks (COFs) are increasingly recognized as promising materials for capturing carbon dioxide due to their large surface areas, adjustable pore sizes, and tunable chemical structures[33]. Recent developments have focused on boosting their performance through targeted functionalization, such as $–SO_3H$, $–NO_2$, OH, and $–NH_2$ to frameworks like COF-300, which significantly enhances their CO_2 adsorption and selectivity. For example, COF-300 modified with $–SO_3H$ can adsorb up to 6.23 $mmol \cdot g^{-1}$ of CO_2 and exhibits a CO_2/N_2 selectivity ratio of 393 under standard conditions[34]. Functionalizing the internal walls of 2D COFs has also proven effective in fine-tuning gas interactions for superior capture efficiency. While these innovations are encouraging, challenges remain in scaling up production, ensuring long-term stability, and integrating these materials into real-world systems. There is also growing interest in developing COF

based composites and applying post-synthetic modifications to improve durability and recyclability.

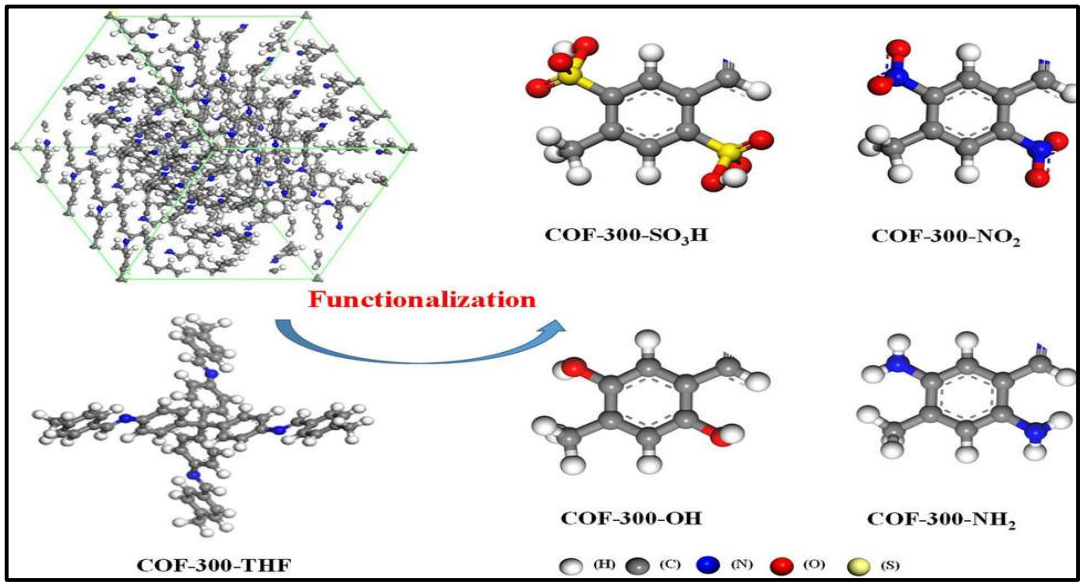

Fig.10 Functionalization of COF-300 for the adsorption of CO_2

1.6.2 COF as Photocatalyst

The efficiency of covalent organic frameworks (COFs) in photocatalysis is heavily influenced by the interplay between their structural crystallinity and chemical stability. While a high degree of crystallinity enhances charge mobility and facilitates effective exciton transport, it can also reduce stability due to the reversible nature of the covalent bonds involved in their construction. On the other hand, improving stability through the use of more rigid linkages, such as β-ketoenamine, may result in decreased structural order, limiting photocatalytic efficiency. To overcome this challenge, researchers have explored various design strategies, including the stabilization of linkages, tuning of interlayer forces, and integration of donor–acceptor motifs to improve exciton separation and charge transfer. Additional enhancements have been achieved through techniques such as heteroatom incorporation, cocatalyst addition, formation of heterojunctions, and morphological tuning like creating nanosheet or hollow architectures to boost light harvesting and catalytic activity[1], [35].

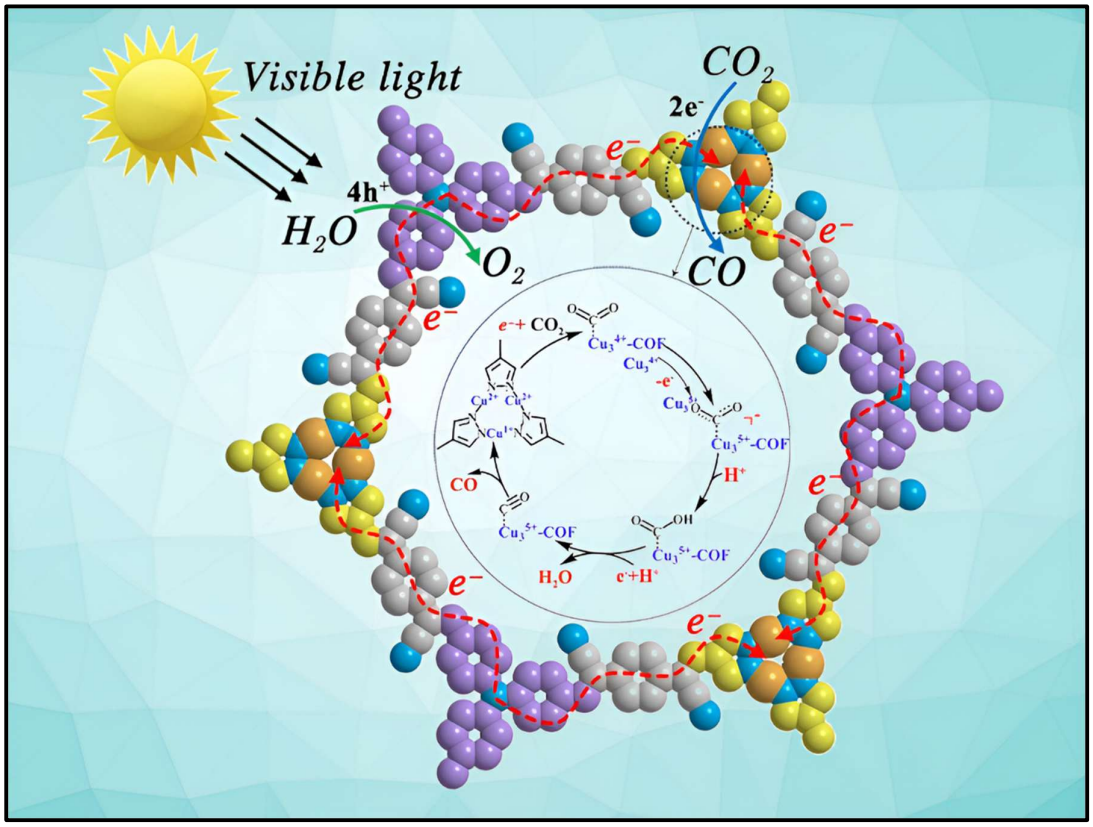

Fig.11 Photocatalytic activity of Covalent Organic Framework[1]

For instance, a COF with enhanced surface crystallinity demonstrated a hydrogen evolution rate of 630 μmol h^{-1} under visible light, attributed to its improved surface structure and internal electric field. These developments highlight COFs as promising materials for applications in photocatalytic hydrogen production and environmental purification..

1.6.3 COF as a Heterogeneous Catalyst in Organic Synthesis

Covalent Organic Frameworks (COFs) are emerging as powerful heterogeneous catalysts in organic synthesis, owing to their customizable architecture, high surface area, and well-defined pore networks. Their ordered, porous structures enable the integration of diverse catalytic sites, which support a wide array of chemical transformations under mild conditions. A key advantage of COFs lies in their capacity to host metal nanoparticles (NPs) within their frameworks. For example, embedding palladium nanoparticles into COFs has shown remarkable effectiveness in cross-coupling reactions[36] like the Suzuki–Miyaura reaction[29]. The uniform distribution of metal NPs within the COF channels promotes catalytic uniformity, improves reaction efficiency, and allows for easy catalyst

separation and reuse[37]. Apart from incorporating external catalytic species, COFs can also be designed to exhibit inherent catalytic activity[38]. The introduction of chiral building blocks into the framework enables the development of chiral COFs, which have been successfully applied in asymmetric synthesis, delivering products with high enantiomeric excess. These materials provide both stability and selectivity, making them highly suitable for stereoselective transformations. Moreover, the tunability of COFs makes them ideal platforms for creating multifunctional catalytic systems.

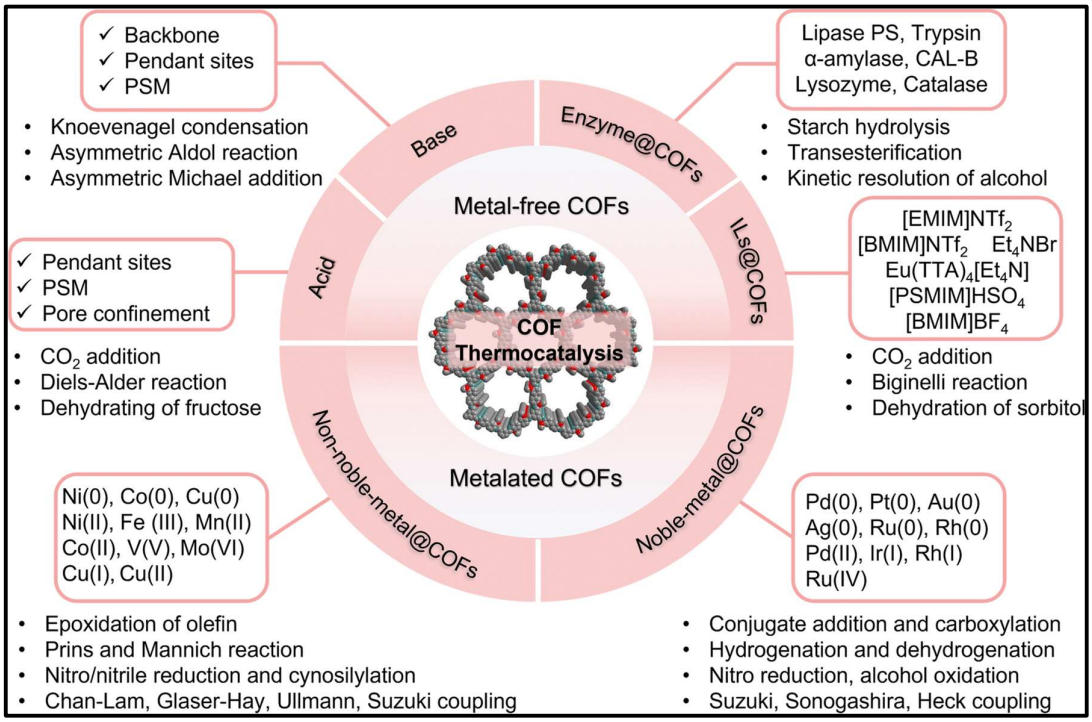

Fig.12 Catalytic activity of COF and metal incorporated COF

Covalent Organic Frameworks (COFs) have emerged as versatile heterogeneous catalysts in organic synthesis, owing to their large surface area, adjustable porosity, and customizable structures. They have been effectively applied in numerous reactions, such as Suzuki–Miyaura cross-coupling using Pd-loaded COFs[29], which exhibit high catalytic activity and reusability. COFs containing amine groups efficiently promote Knoevenagel condensation under gentle conditions, while those incorporating proline enable asymmetric aldol reactions with notable selectivity[39]. Furthermore, COFs have shown excellent performance in oxidation processes like the conversion of sulfides to sulfoxides[40]

CHAPTER-2

Synthesis and Characterization of CTN & Cu(II)@CTN Covalent Organic Framework

2. SYNTHESIS OF Cu(II) IMMOBILIZED CTN COVALENT ORGANIC FRAMEWORK

2.1 Hydrazone-linked Covalent Organic Framework

Hydrazone-linked Covalent Organic Frameworks (COFs) are porous, crystalline materials formed through the reversible reaction between hydrazide and aldehyde building blocks, resulting in hydrazone (-C=N–NH-) bonds. These linkages contribute to the material's structural regularity and adjustable pore characteristics, while also providing superior resistance to hydrolysis and chemical degradation. The reversible nature of hydrazone bonds allows for self-correction during framework formation, aiding in the development of highly ordered structures.

Key Characteristics

Thermal Resistance:

Such COFs are known for their thermal robustness, making them suitable for operations in elevated temperatures and demanding conditions.

Enhanced Chemical Durability:

Compared to imine-linked COFs, hydrazone-linked frameworks exhibit improved resistance to chemical degradation and hydrolysis, particularly in acidic or aqueous conditions.

High Porosity and Adjustable Surface Area:

Hydrazone-linked COFs maintain the high surface area and customizable pore size typical of COFs, making them highly effective for gas storage, separation, and catalytic applications.

Heterogeneous Catalyst:

The chemical and thermal stability of the hydrazone based covalent organic framework make the substance excellent choice for using it as a catalyst in various reactions.

To synthesize the hydrazone-linked Covalent Organic Framework (COF) named CTN COF, we selected benzene-1,3,5-tricarbohydrazide (BTH), which was synthesized from benzene-1,3,5-tricarboxylic acid and 4,4',4''-((1,3,5-triazine-2,4,6-triyl)tris(oxy))tribenzaldehyde (TTTB) from the reaction of Cyanuric chloride and 4-Hydroxybenzaldehyde, as the building blocks. These precursors were chosen due to their ability to form robust hydrazone linkages, as well as their excellent thermal and chemical stability. The resulting framework benefits from the structural rigidity and functional diversity of both monomers, which contribute to the overall performance of the COF in demanding chemical environments. And the process that we have chosen is solvothermal synthesis by using o-DCB and Butanol as mixture of solvent(1:1).

2.2 Experimental Section:

2.2.1 Materials:

All the required chemicals, Benzene-1,3,5-tricarboxylic acid, 2,4,6-trichloro-1,3,5-triazine,4-Hydroxybenzaldehyde, Butanol, o-DCB, and Cupric acetate, were used without further purification and bought from commercial sources. The reaction was carried out in an autoclave, and a centrifuge was used to separate the COF from the solvent. The COF was washed several times with solvents of different polarities like DMF, Dioxane, Acetonitrile, and Acetone. Similarly Cu(II)-CTN was washed with Methanol.

2.2.2 Synthesis of BTH & TTTB (Linkers)

Benzene-1,3,5-tricarboxylic acid was refluxed with methanol and catalytic sulfuric acid for 10–12 hours to yield trimethyl benzene-1,3,5-tricarboxylate. After removing the solvent under reduced pressure, the ester intermediate was dissolved in methanol and reacted with excess hydrazine hydrate at room temperature for 12 hours. The mixture was stirred to complete the conversion to hydrazide groups, and the solvent was evaporated. The resulting crude product was purified by recrystallization to obtain benzene-1,3,5-tricarbohydrazide.

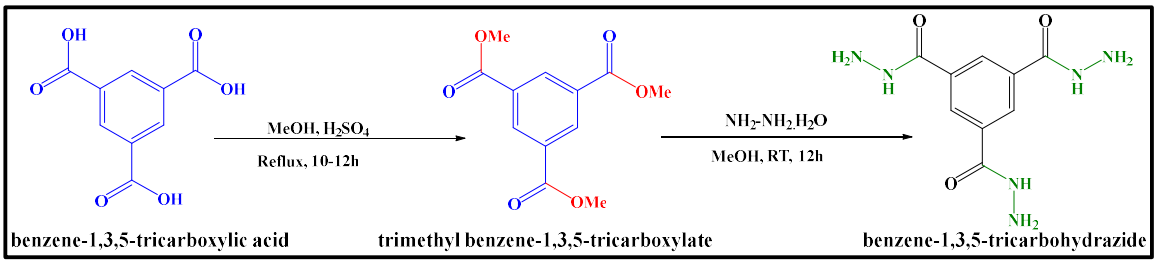

Scheme 1: Synthesis of linker benzene-1,3,5-tricarbohydrazide

The 2nd building unit i.e. TTTB, is prepared when 2,4,6-Trichloro-1,3,5-triazine and 4-hydroxybenzaldehyde were reacted in the presence of sodium carbonate (Na_2CO_3) in 1,4-dioxane as the solvent. The mixture was refluxed for 20 hours to facilitate the substitution of chlorine atoms with 4-hydroxybenzaldehyde groups. After completion of the reaction, the product was isolated and purified to afford the target compound, **TTTB**, in a yield of 79%.

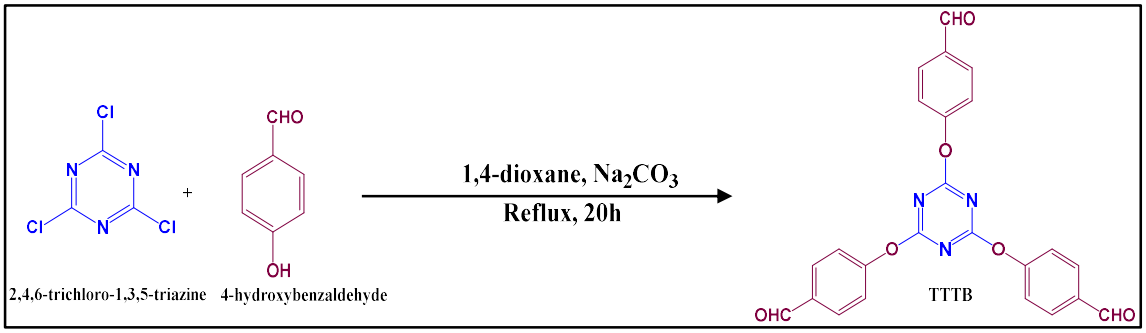

Scheme 2: Synthesis of linker TTTB

2.2.3 Synthesis of CTN COF

In a 25 mL autoclave, benzene-1,3,5-tricarbohydrazide (BTH) (1mmol,1eq.) and 4,4',4''-((1,3,5-triazine-2,4,6-triyl)tris(oxy))tribenzaldehyde (TTTB) (1mmol,1eq.) were dissolved in dissolved in 5mL of a mixture of Butanol and o-DCB in the ratio 1:1. To this solution 400microL of 6M Acetic acid was added, and again sonicated for 5min. The resulting mixture was then subjected to a solvothermal reaction by enclosing it and heating at 120 °C for 72 hours under a nitrogen atmosphere to ensure an inert environment and facilitate the reaction. After the reaction period, the resulting mixture was allowed to cool, then centrifuged and washed with DMF, Dioxane, Acetonitrile, and Acetone to eliminate any unreacted starting materials or oligomers in the COF.

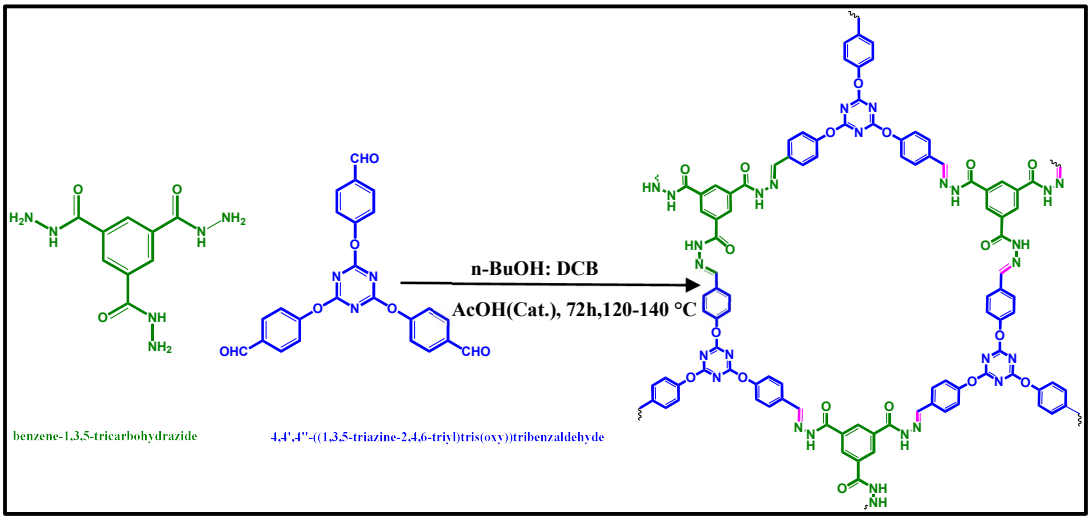

Scheme 3: Synthesis of CTN Covalent Organic Framework

2.2.4 Post-Synthetic Incorporation of Cu(II) into CTN COF

To achieve post-synthetic metalation, 250 mg of CTN COF was dispersed in methanol (15 mL) in a 25 mL round-bottom flask. Then 50mg of Cupric acetate monohydrate [$Cu(OAc)_2 \cdot H_2O$] was added to the suspension, and the mixture was stirred continuously at room temperature for 24 hours to enable effective coordination of Cu(II) ions within the COF matrix. Following the reaction, the solid material was separated by centrifugation and washed several times with fresh methanol to remove excess, unbound copper species. The resulting greenish-yellow solid was dried under vacuum and designated as Cu(II)@CTN COF.

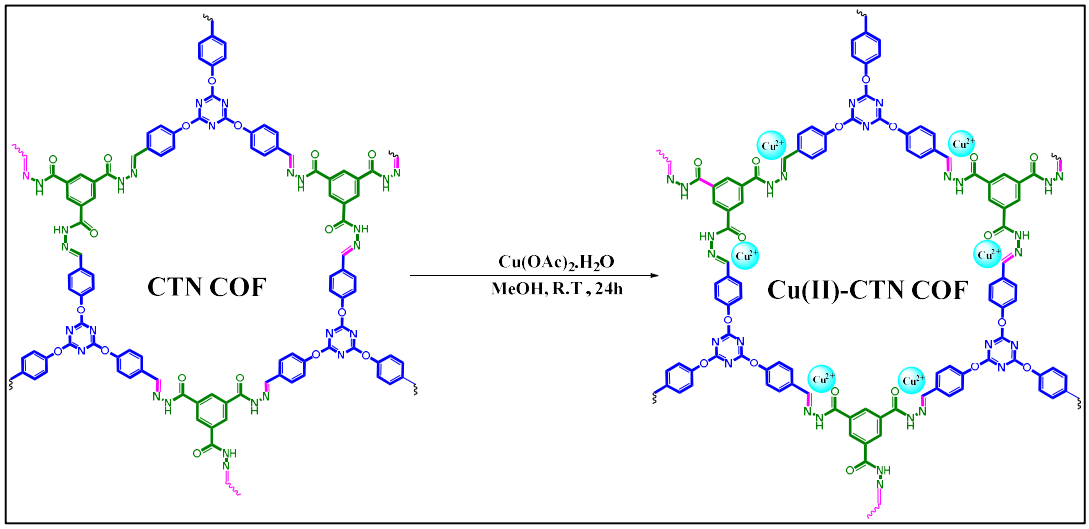

Scheme 4: Incorporation of Cu(II) into the CTN COF

2.3 Characterization of CTN COF and Cu(II)@CTN COF

2.3.1 FT-IR Analysis

The successful synthesis of CTN COF was confirmed by FT-IR spectroscopy, as shown in **Fig. 13** which illustrates key changes in vibrational bands resulting from the condensation between benzene-1,3,5-tricarbohydrazide and TTTB. In the spectra of the starting monomers, the $-NH_2$ stretching vibrations are observed in the 3330–3430 cm^{-1} region, while the hydrazide C=O stretching appears at approximately 1624 cm^{-1}. The aldehyde component (TTTB) exhibits a strong C=O stretch around 1700–1720 cm^{-1}. Upon formation of the COF, these characteristic bands disappear or significantly reduce in

intensity, indicating complete consumption of both amine and aldehyde groups during the reaction.

A new absorption band appears in the 1654–1660 cm^{-1} range, corresponding to the C=O stretch of the acyl hydrazone linkage. This shift from the original hydrazide carbonyl frequency is attributed to resonance stabilization and electron delocalization in the newly formed imine-type (C=N–N) bond. Additionally, a peak near 1605–1620 cm^{-1} is assigned to the C=N stretching vibration, directly confirming the formation of hydrazone linkages. The broad band near 3280 cm^{-1}, associated with N–H stretching, replaces the sharper NH_2 signals seen in the monomers, further supporting the structural transformation. In the Cu(II)@CTN COF spectrum, subtle broadening and shifts in the N–H and C=O regions are observed, suggesting coordination between Cu(II) ions and donor atoms (nitrogen or oxygen) of the framework. These changes indicate alterations in the electronic environment due to metal binding. Overall, the FT-IR analysis (Figure 13) provides strong evidence for successful hydrazone linkage formation and effective post-synthetic incorporation of Cu(II) into the COF structure.

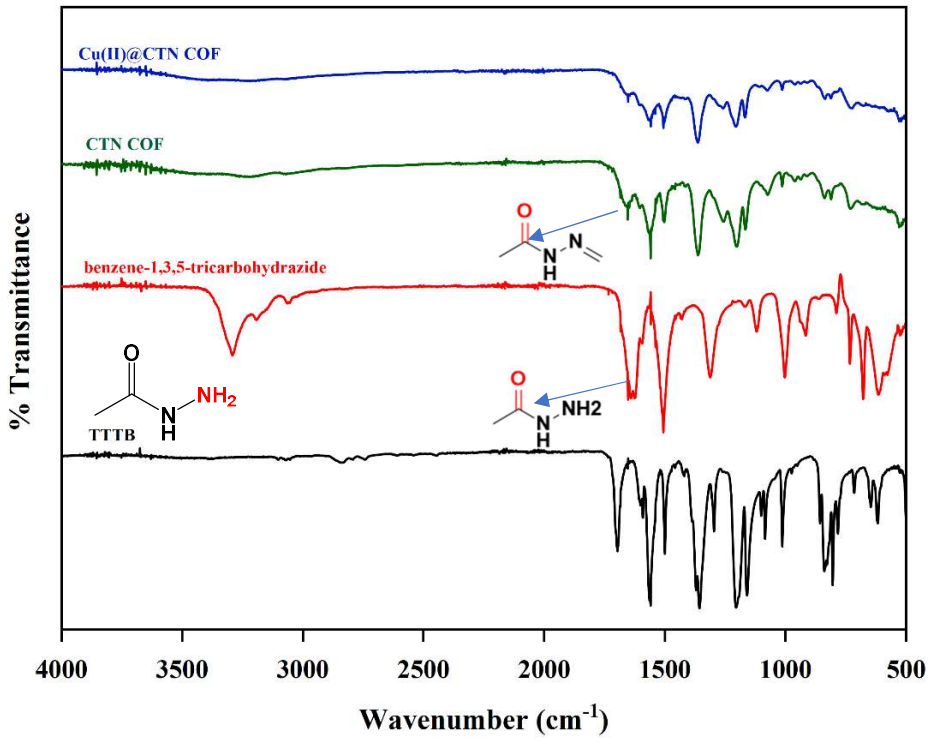

Fig. 13 Comparative FT-IR analysis of a) TTTB, b) BTH, c) CTN COF, d) Cu(II)@CTN COF

2.3.2 P-XRD Analysis

Powder X-ray diffraction (PXRD) analysis **Fig.14** was conducted to verify the successful synthesis of CTN-COF from its building units, BTH and TTTB, and to investigate the subsequent incorporation of Cu(II) ions into the framework. As illustrated in Figure 14, the PXRD patterns of the individual linkers BTH and TTTB exhibit sharp and distinct peaks in the low-angle region, reflecting their high crystallinity. Following the polymerization reaction, the resulting CTN-COF displays a broadened diffraction pattern, indicative of reduced crystallinity. This broadening is typical for COFs synthesized under solvothermal conditions and signifies the formation of an extended, yet partially amorphous, covalent network. After metalation of the CTN-COF with a Cu(II) precursor, the PXRD pattern of Cu(II)-CTN-COF reveals two additional peaks at 2θ values of 14.45° and 43.4°, which are not observed in either the pristine COF or the linker materials.

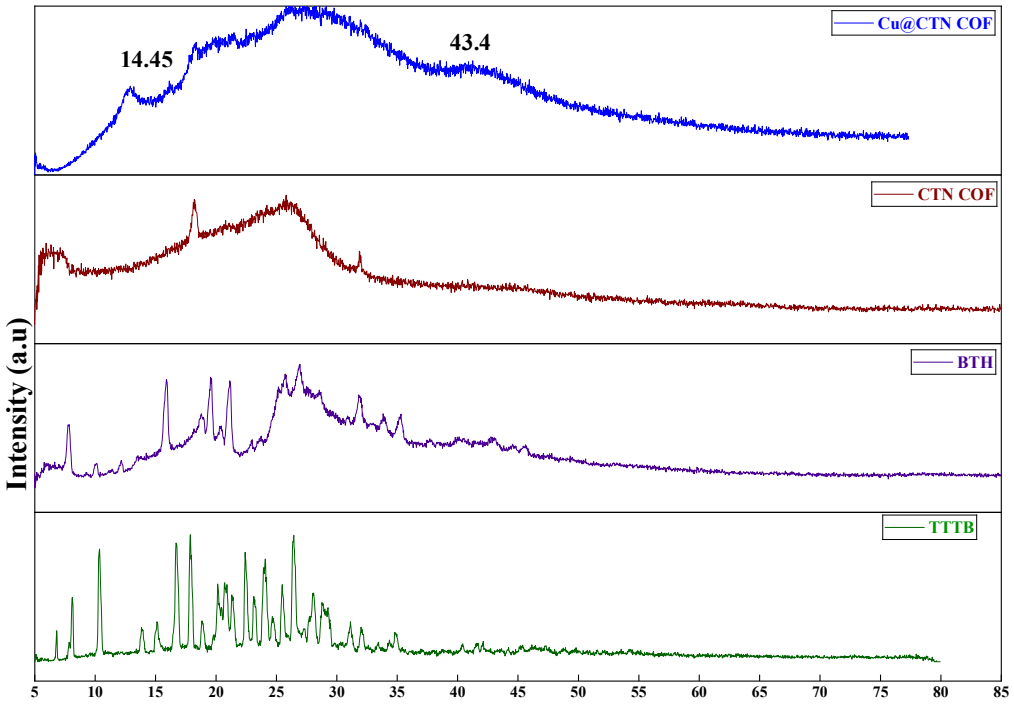

Fig. 14 Comparative P-XRD analysis of a)TTTB, b) BTH, c) CTN COF, d) Cu(II)@CTN COF.

The appearance of the peak at 14.45° suggests a structural rearrangement within the COF, potentially arising from coordination interactions between Cu(II) ions and donor atoms (e.g., nitrogen or oxygen) in the framework. Meanwhile, the peak at 43.4° is likely

attributable to the formation of small, crystalline Cu-containing domains embedded within the COF matrix. These new diffraction features confirm the successful incorporation of Cu(II) into the COF structure. Importantly, the retention of the broad features associated with CTN-COF indicates that the overall framework remains largely preserved after metalation, with the Cu(II) ions effectively coordinated within the porous architecture.

To gain further insight into the long-range order and crystallinity of the synthesized CTN-COF, low-angle PXRD analysis was performed **(Figure 15).** The pattern reveals a distinct diffraction peak at approximately $2\theta \approx 2.5\text{-}3.5°$, which corresponds to the (100) reflection plane. This feature is characteristic of 2D layered COFs and indicates periodic ordering in the framework, most likely arising from π–π stacking and the regular arrangement of building units within the 2D layers.

The presence of the (100) peak, albeit broad and of low intensity, suggests that CTN-COF exhibits a certain degree of structural order in the in-plane direction, typical of many amorphous-to-semicrystalline COFs synthesized under solvothermal conditions.

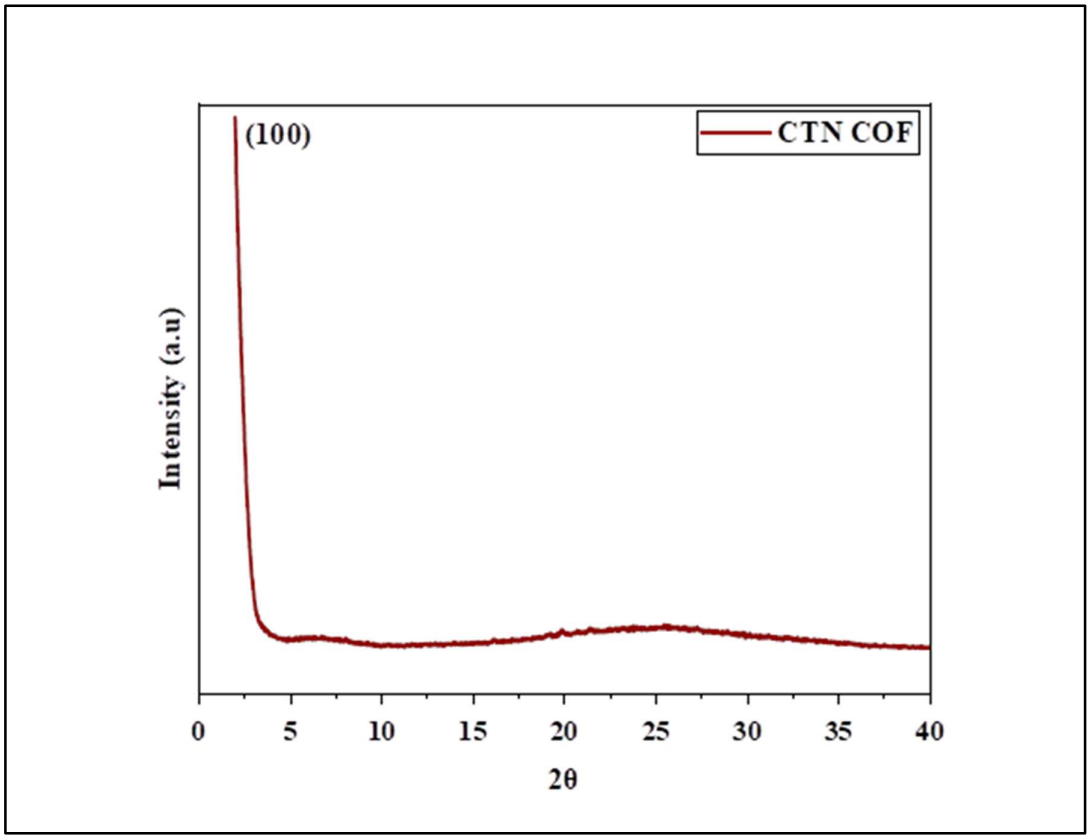

Fig. 15 Low angle P-XRD Analysis of CTN COF

2.3.3 Thermogravimetric Analysis

The thermal stability of CTN COF and its Cu(II)-loaded counterpart was assessed via thermogravimetric analysis **(Figure 16).** The pristine CTN COF shows excellent thermal resistance, with an initial weight retention of ~88.1% up to 338.8 °C, and a significant degradation step occurring around 402 °C. In contrast, Cu(II)@CTN COF displays an earlier onset of decomposition with 73.1% weight retained at the same temperature, indicating slightly reduced thermal stability upon metal loading. This decrease in thermal resistance can be attributed to the disruption of the framework integrity due to Cu(II) coordination, which may weaken the covalent network. Nevertheless, both materials exhibit high thermal robustness, affirming their suitability for applications requiring stability at elevated temperatures.

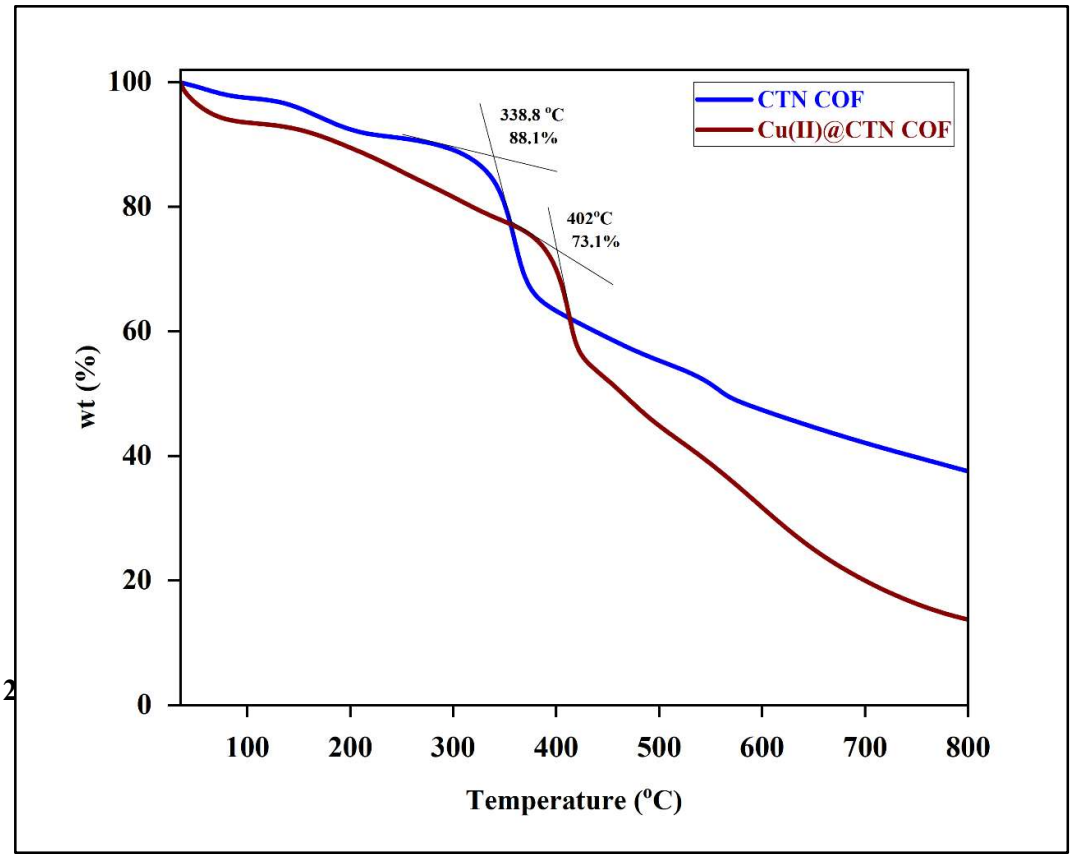

Fig. 16 Thermogravimetric Analysis of CTN COF and Cu(II)@CTN COF

2.3.4 Brunauer-Emmett-Teller (BET) surface area analysis

The Nitrogen adsorption–desorption isotherms presented in the figure provide insight into the surface characteristics of both the pristine CTN COF (**Fig.17b**) and the Cu(II)-incorporated CTN COF (**Fig.17b**).For the original CTN COF, the BET surface area is measured at 22.506 m^2/g, with a pore volume of 0.149048 cc/g and an average pore radius of 2.60071 nm. These values indicate a mesoporous structure with relatively high surface area, which is beneficial for applications like adsorption or catalysis.

After the incorporation of Cu(II), there is a noticeable decrease in porosity. The surface area reduces to 12.4291 m^2/g, the pore volume drops to 0.0332538 cc/g, and the pore radius becomes 1.87251 nm. This reduction suggests that the introduction of Cu(II) ions likely occupies or blocks some of the pores within the framework, thereby lowering the available surface area and pore size. This structural modification implies that Cu(II) coordination not only alters the physical texture but may also influence the material's accessibility and interaction with guest molecules. Such changes are critical for understanding the material's behaviour in practical applications, particularly in catalysis, separation, or sensing processes.

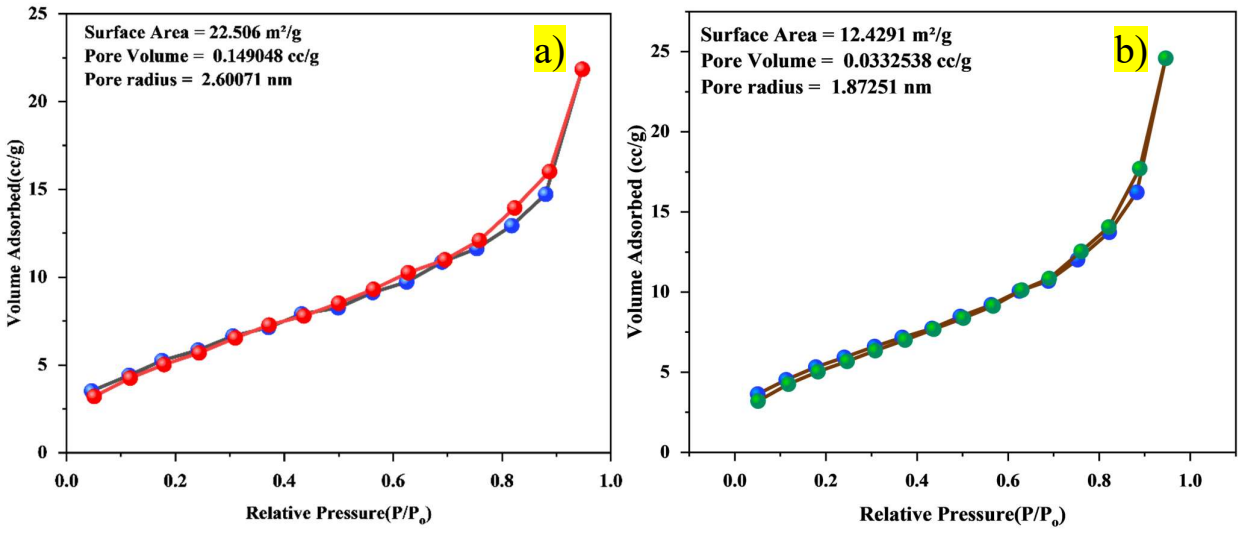

Fig. 17 BET isotherms of a) CTN COF b) Cu(II)@ CTN COF

2.3.5 Field Emission Scanning Electron Microscope (FE-SEM) Analysis of CTN COF

Figure **18 (a,b,c)** presents the scanning electron microscopy (SEM) image of the synthesized COF recorded at 10000x and 30,000x magnification.

- Surface Features: The surface of the rods appears relatively smooth and uniform, with no significant surface roughness or aggregation visible at this magnification. This smoothness may reflect a well-ordered crystalline framework and minimal structural defects**.**
- Morphology: The material exhibits a rod-like or cylindrical morphology, suggesting an anisotropic growth pattern likely guided by the directional nature of the covalent linkages during framework formation.
- Structural Arrangement: The rods are closely packed and partially entangled, suggesting good material continuity and possible inter-particle interactions that may enhance mechanical integrity and stability.
- Aggregation: Some degree of particle agglomeration is observed, which is common for COFs synthesized via solvothermal methods, potentially due to hydrogen bonding and π–π stacking interactions.

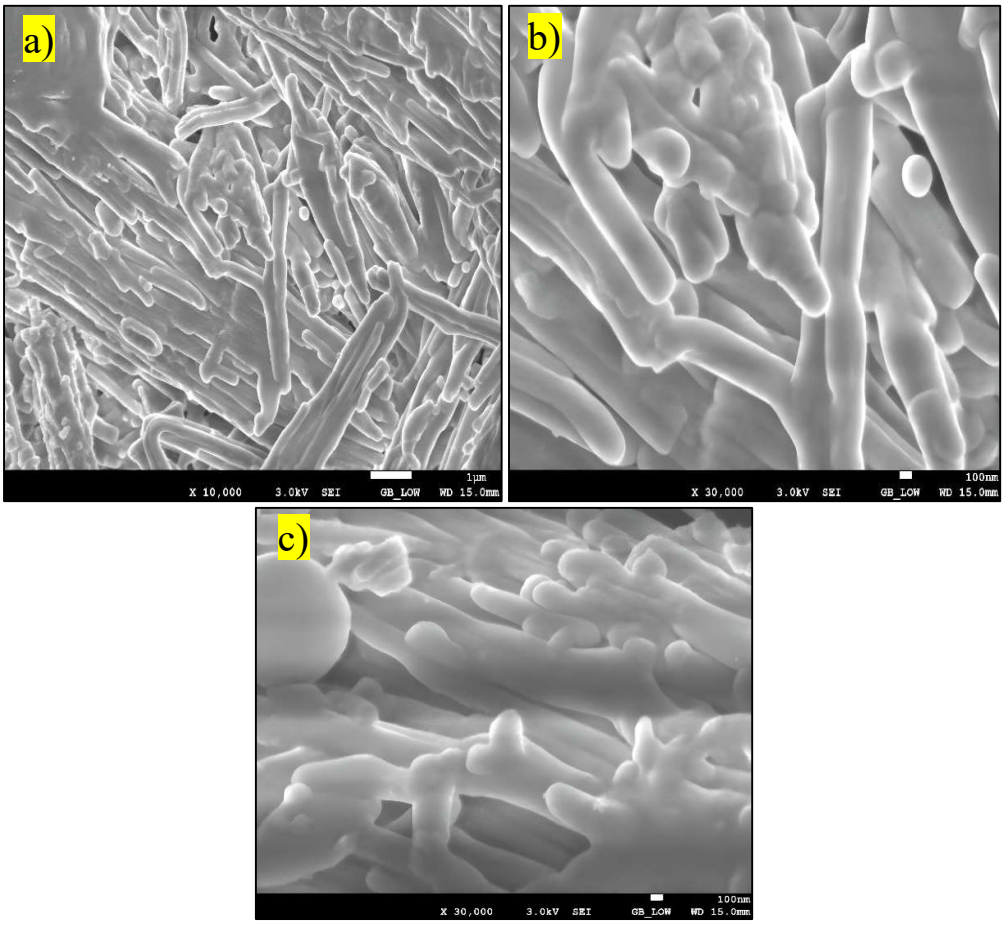

Fig. 18 FE- SEM Images of CTN COF

2.3.6 Field Emission Scanning Electron Microscope (SEM) Analysis of Cu(II)-CTN COF

Figure 19(a,b) presents the scanning electron microscopy (FE-SEM) image of the synthesized Cu(II)-COF recorded at 5000x and 10,000x magnification.

Morphology:

The FE-SEM images display a preserved rod-like morphology similar to the pristine CTN COF, indicating that post-synthetic metalation did not disrupt the overall framework structure. However, additional surface roughness and granular features are observed after Cu(II) incorporation.

Surface Features:

The surface of the Cu(II)@CTN COF appears more irregular and decorated with spherical and amorphous deposits, suggesting successful coordination or anchoring of Cu(II) ions onto the COF structure. These features reflect enhanced surface heterogeneity due to metal incorporation.

Particle Size and Aggregation:

The presence of spherical particles may also indicate localized Cu(II) complex formation or aggregation on the COF surface.

Structural Integrity:

Despite the post-synthetic modification, the framework retains its overall integrity without significant collapse, which confirms the robustness and chemical stability of the COF backbone upon metalation.

Furthermore, the average particle size of the Cu(II)@CTN COF was found to be 287.28nm.

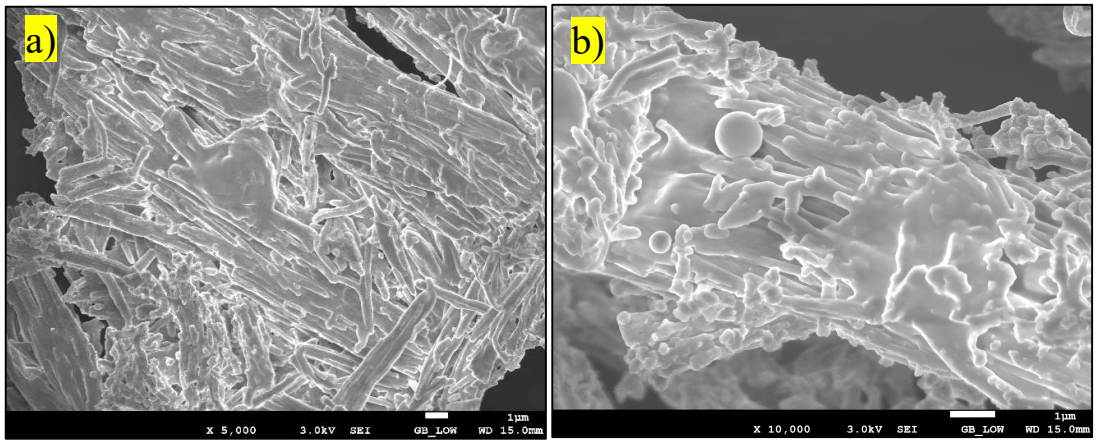

Fig.19 FE- SEM Images of Cu(II)@CTN COF

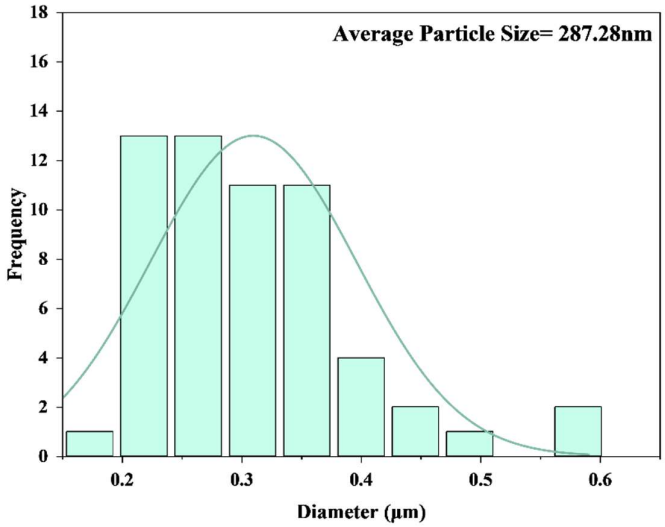

Fig. 20 Particle distribution curve of Cu(II)@CTN COF

2.3.7 EDS Analysis and Elemental Mapping

Pristine CTN COF: The EDS spectrum of the unmodified CTN COF displays signals for carbon (C), nitrogen (N), and oxygen (O), with surface atomic percentages of C: 62.7%, O: 21.0%, N: 16.9%. Trace platinum (Pt) peaks observed are attributed to the sample stub.

Elemental mapping confirms a uniform distribution of the detected elements across the COF surface, suggesting a well-formed and compositionally homogeneous porous framework.

Cu(II)-Incorporated CTN COF: After Cu(II) incorporation, EDS analysis reveals new copper (Cu) signals, along with C: 51.5%, O: 21.2%, N: 10.4%, Cu: 6.0% as surface atomic percentages.

Elemental mapping images show an even distribution of Cu throughout the analysed region, indicating successful dispersion of the metal within the COF structure. The slight decrease in surface nitrogen content implies possible interaction or coordination between Cu(II) and nitrogen sites within the framework. Hence, the results confirm the successful synthesis of the CTN COF and the effective incorporation of Cu(II) into its framework. The uniform elemental distributions observed in mapping images, combined with the emergence of copper peaks in the EDS spectrum, indicate that Cu(II) ions are well-dispersed on the COF surface. These findings support the structural integrity and potential functionality of the Cu-modified COF for further application studies.

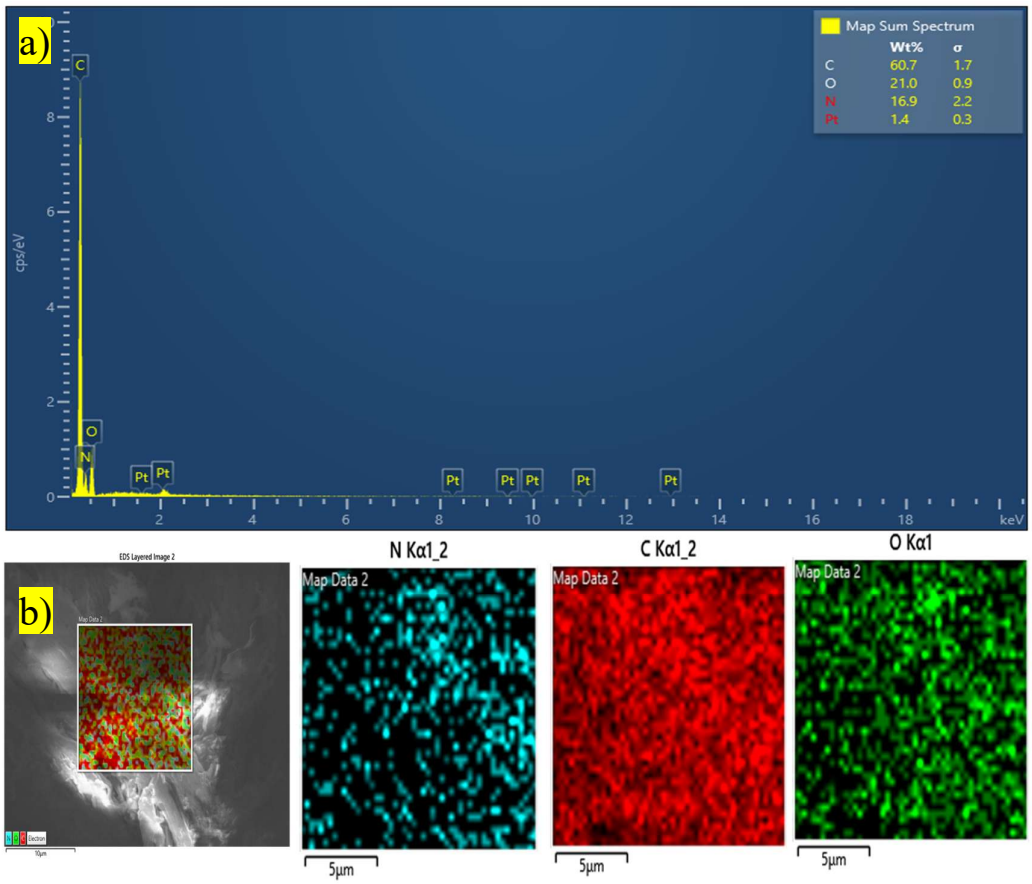

Fig.21 EDS(a) and Elemental analysis(b) of CTN COF

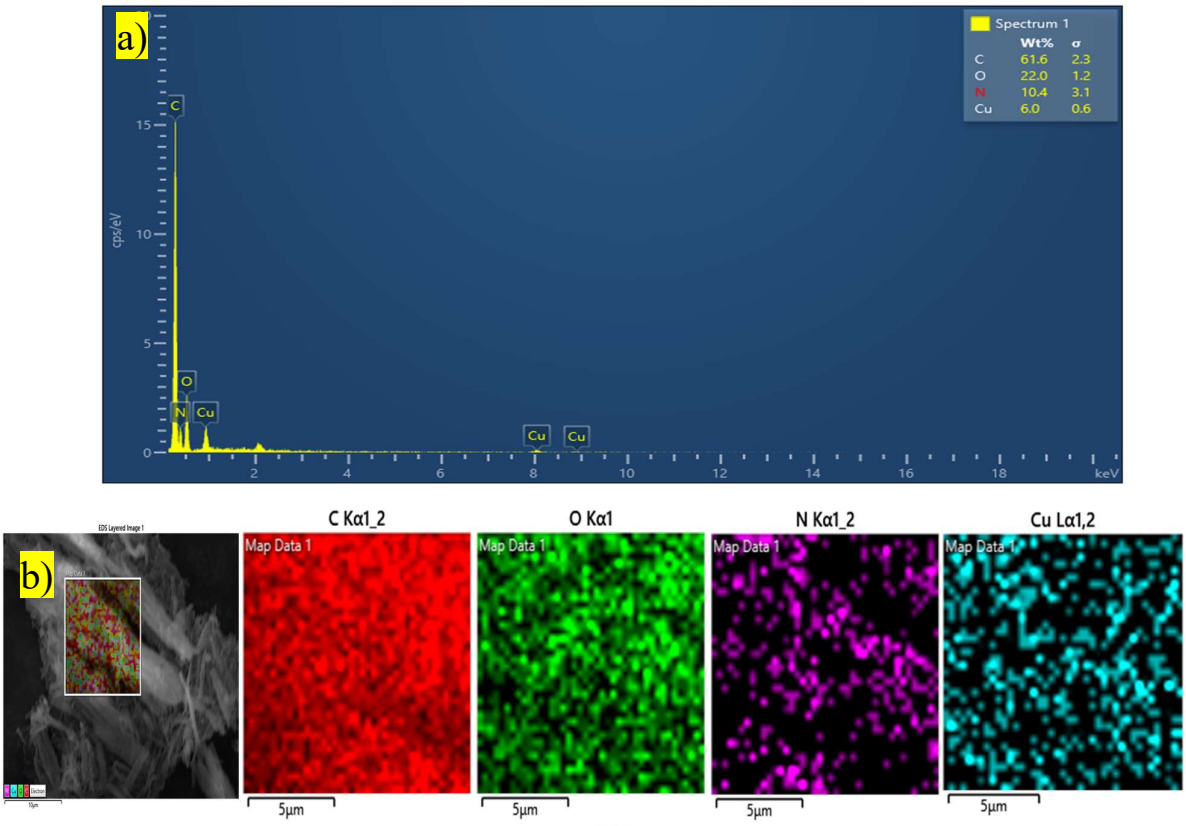

Fig. 22 EDS(a) and Elemental analysis(b) of Cu(II)-CTN COF

2.3.8 X-ray photoelectron spectroscopy (XPS)

Figure **23(a)** represents the X-ray photoelectron spectroscopy (XPS) analysis, revealing the elemental surface composition of Cu(II)-CTN COF with prominent peaks corresponding to Cu, C, N, and O. This elemental distribution aligns well with the results previously observed in the EDS analysis. In the C1s spectrum **Fig. 23(b)** of the synthesized Cu(II)@CTN COF displays three deconvoluted peaks are observed, the peaks at 284.6 eV and 286.1 eV are attributed to C–C or C=C bonds typically found in aromatic structures and C=N bonds associated with hydrazone linkage found in the Cu(II)@CTNCOF[41]**.** The N1s spectrum shown in **Fig. 23(c)** can be deconvoluted into two distinct peaks located at 398.5 eV and 399.7 eV, corresponding to (C=N–C) linkages and amine groups (C–NH–C) of the catalyst, respectively [42], [43]. In the O1s spectra shown in **Fig. 23(d)**, the peak observed around 531.6 eV corresponds to the oxygen in carbonyl groups (C=O) with minimal variation in binding energy, while the peak at 533.0 eV is associated with surface-adsorbed water molecules [42], [43].

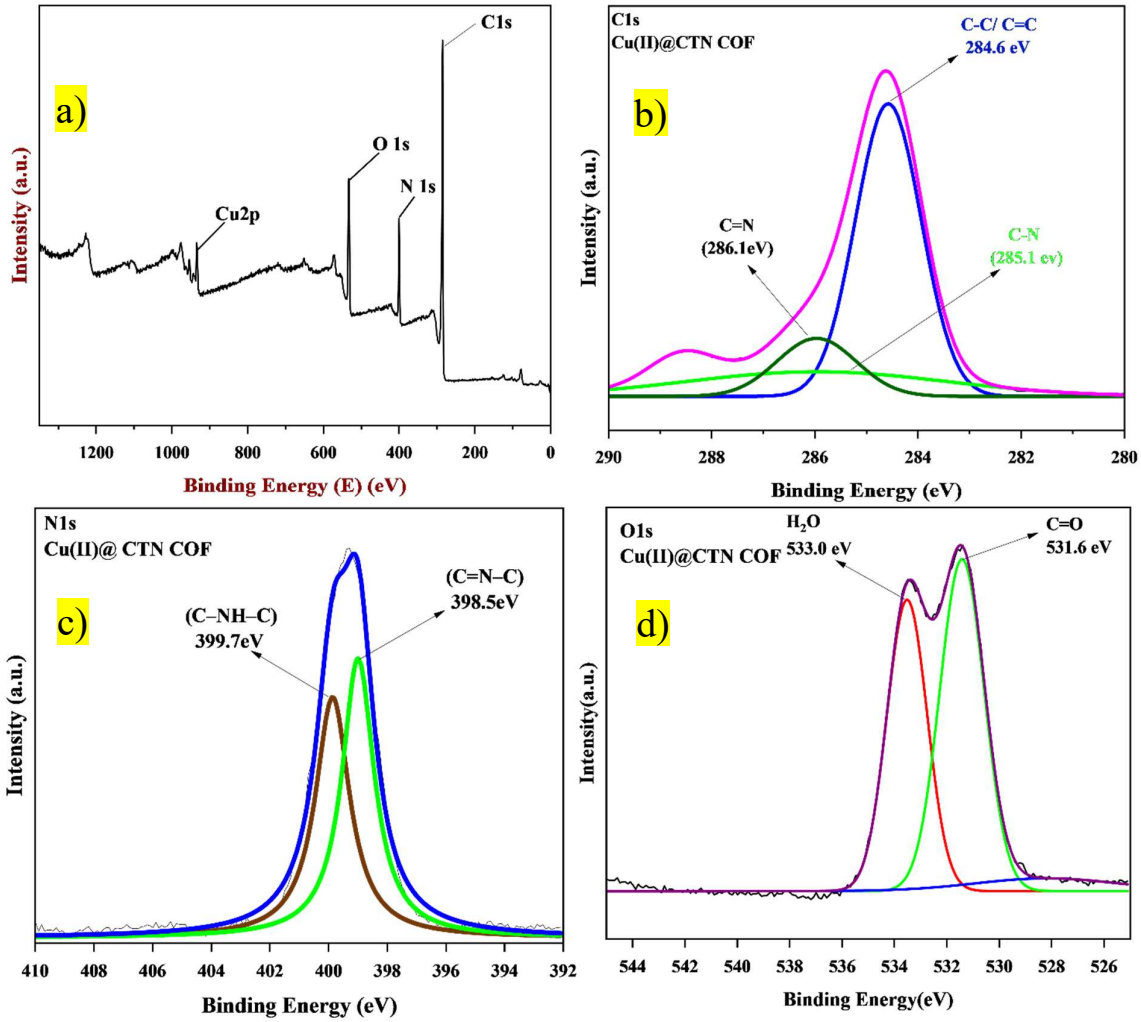

Fig. 23 XPS Analysis of Cu(II)@CTN COF . a) High resolution full XPS survey, b) C1s Spectra, c) N1s Spectra, d) O1s Spectra

The XPS wide scan spectrum **Fig. 24** indicates the presence of key elements, including copper, oxygen (O1s), nitrogen (N1s), and carbon (C1s) on the surface of the synthesized CTN COF. In the case of Cu(II)@CTN COF, the fitted XPS data show distinct peaks for Cu $2p_{3/2}$ at 933.6 eV and Cu $2p_{1/2}$ at 954.0 eV. Additionally, prominent satellite features observed near 944 eV and around 962 eV further support the assignment to Cu^{2+}, as these shake-up peaks are a hallmark of the $3d^9$ electron configuration associated with this oxidation state.

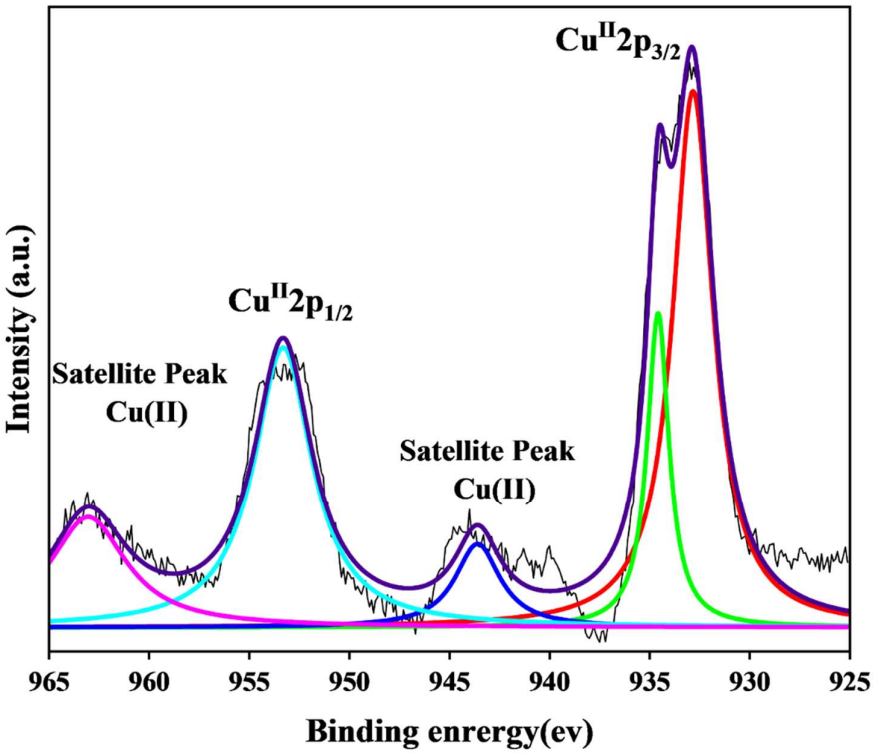

Fig. 24 High resolution Full XPS survey of Cu 2p

This spectral profile is consistent with copper(II) complexes, such as copper(II) acetate, where copper is typically coordinated to oxygen-donor ligands.

CHAPTER-3

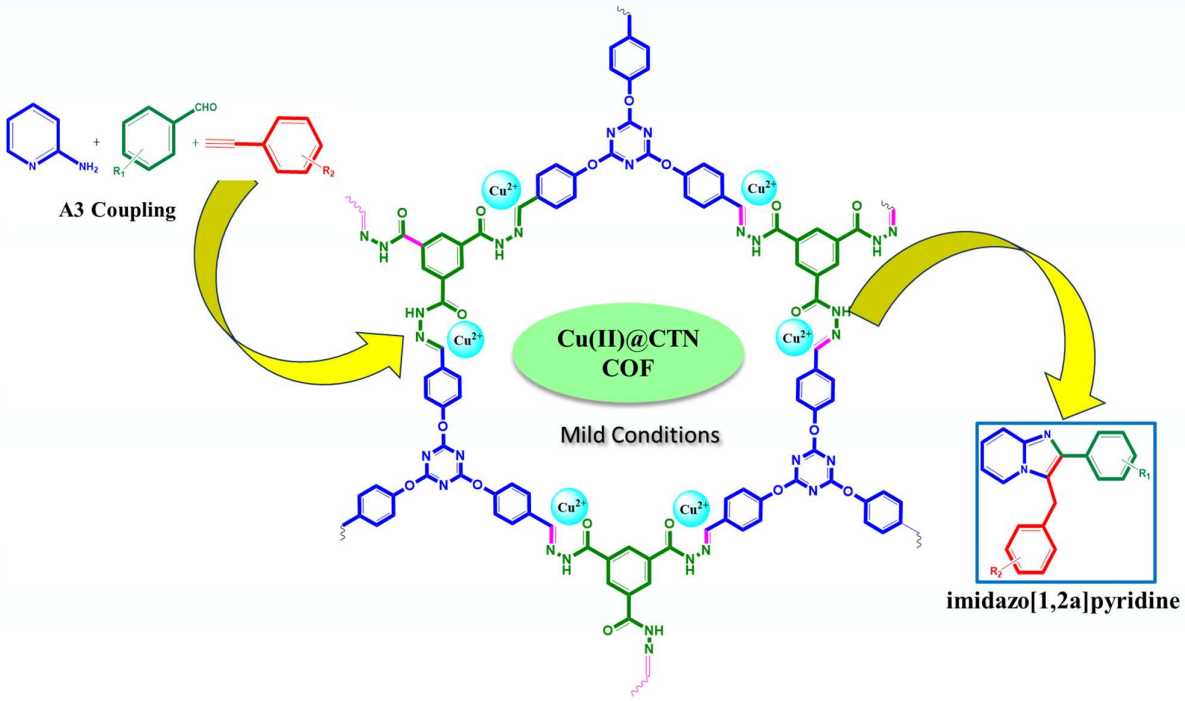

Catalytic application of Cu(II)-CTN COF as a Efficient and Recyclable Catalysts for Sustainable Synthesis of Imidazo[1,2-a]pyridines

3.1 Introduction about Imidazo[1,2-a]pyridines

Imidazo[1,2-a]pyridines represent a well-established class of fused heterocyclic compounds that have attracted substantial attention in medicinal chemistry. Their development has been driven largely by their potent biological activities, especially within the central nervous system. Their synthesis and structural modifications have been intensively explored since the 20th century, particularly due to the success of several imidazo[1,2-a]pyridine-based drugs in clinical use. Imidazo[1,2-a]pyridines are pharmacologically versatile, with a wide range of biological activities [44]as follows:

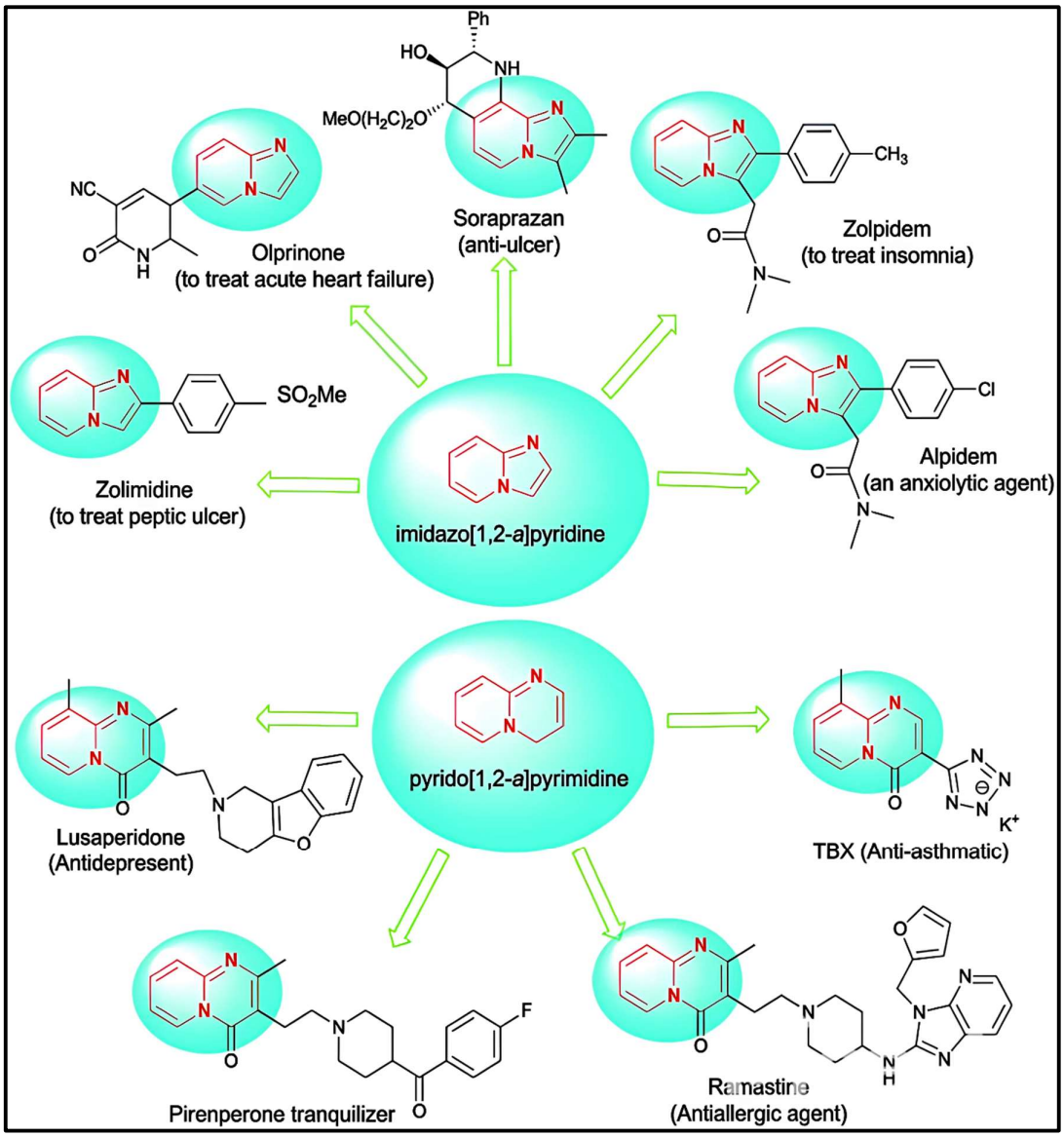

Fig.24 Potent biological activity of Imidazo[1,2-a]pyridines

- CNS Activity: Compounds like Zolpidem and Alpidem exemplify their strong action on the CNS(Central Nervous System), being used as hypnotics and anxiolytics, respectively[45]
- Cardiovascular Effects: Molecules such as olprinone are employed for their role in treating acute heart failure[46], [47], likely through phosphodiesterase inhibition.
- Antimicrobial Properties: Many derivatives display antibacterial and anti-inflammatory effects, positioning them as candidates for treating infections and inflammatory disorders[48], [49], [50].

Hence, this heterocyclic scaffold forms the core of many approved and investigational drugs, underscoring its utility in drug development. The flexibility in substitution on both the imidazole and pyridine rings allows for tuning of pharmacodynamic properties.

Recent reports on the synthesis of imidazo[1,2-a]pyridines have documented several efficient methodologies. The Groebke–Blackburn–Bienaymé (GBB) multicomponent reaction[51], involving 2-aminopyridines, aldehydes, and isocyanides, is a well-established and frequently used approach. Additionally, transition-metal-catalyzed cyclizations employing Pd[52], Cu[53], or Fe[54] have been widely reported for constructing the imidazo[1,2-a]pyridine core with structural diversity. Other documented methods include photocatalytic and electrochemical syntheses, which offer alternative, milder routes to these heterocycles. These strategies form the basis for ongoing exploration in heterocyclic and medicinal chemistry.

Additionally recent times a variety of strategies have been explored for constructing imidazo[1,2-a]pyridine frameworks. Nonetheless, many of these methods suffer from drawbacks such as limited applicability or the necessity of multi-step synthesis of precursors [55], [56]. Among the various approaches, multicomponent reactions (MCRs) stand out due to their efficiency, cost-effectiveness, and eco-friendly nature. These reactions typically require less time, lower energy input, and affordable starting materials, offering both economic and environmental advantages [57], [58]. One particularly promising MCR involves the combination of pyridine-2-amines, aldehydes, and terminal alkynes, which has proven to be an effective route for synthesizing imidazo[1,2-a]pyridines. This method has been successfully implemented using a range of metal-based

catalysts, such as CuCl/$Cu(OTf)_2$ [59], $CuSO_4$/$TsOH \cdot H_2O$[59], $InBr_3$[60], CuI supported on $NaHSO_4 \cdot SiO_2$[61], and a $CuSO_4$/glucose system[62]

In this context, we have developed a novel and sustainable synthetic method or route for preparing imidazo[1,2-a]pyridine derivatives via a copper-catalysed cyclization reaction. The reaction begins with a condensation of 2-aminopyridine (1 eq) with an aldehyde and an alkyne derivative in the presence of a copper(II) catalyst (Cu(II)@CTN COF) under reflux conditions (110-120°C for 6 hours) in toluene. The process proceeds through a 5-exo-dig cyclization mechanism followed by a 1,3-prototropic shift, resulting in the desired imidazo[1,2-a]pyridine structure. This approach offers a robust and efficient synthetic pathway to access functionalized imidazo[1,2-a]pyridines with diverse substituents, useful for various medicinal and material applications. The reaction conditions ensure good yields and high regioselectivity, demonstrating the potential of this method in the development of new bioactive compounds.

3.2 Results and Discussion

In this study, we synthesized a diverse series of imidazo[1,2-a]pyridine derivatives via a one-pot, three-component reaction. The protocol utilized either 2-aminopyridine, various substituted aromatic aldehydes, and aryl alkynes under the catalytic influence of Cu(II)@CTN COF in refluxing conditions for 6 hours. The reaction proceeds through initial condensation between 2-aminopyridine and the aldehyde to form an propargyl amine intermediate, which undergoes further coupling with the alkyne component. This is followed by a 5-exo-dig cyclization and 1,3-prototropic shift, leading to the formation of the imidazo[1,2-a]pyridine core. The use of the Cu(II)@CTN COF catalyst facilitated efficient cyclization and improved yields while also aligning with green chemistry principles by allowing catalyst recyclability. The methodology showed broad substrate scope, tolerating various electron-donating and electron-withdrawing groups on both the aldehyde and alkyne components. Products were obtained in good to excellent yields, and the structures were confirmed via spectral data (NMR, IR, and MS), consistent with the expected framework. This reaction strategy demonstrates a practical and eco-friendly approach for constructing biologically relevant imidazo[1,2-a]pyridine scaffolds with potential applications in pharmaceutical chemistry.

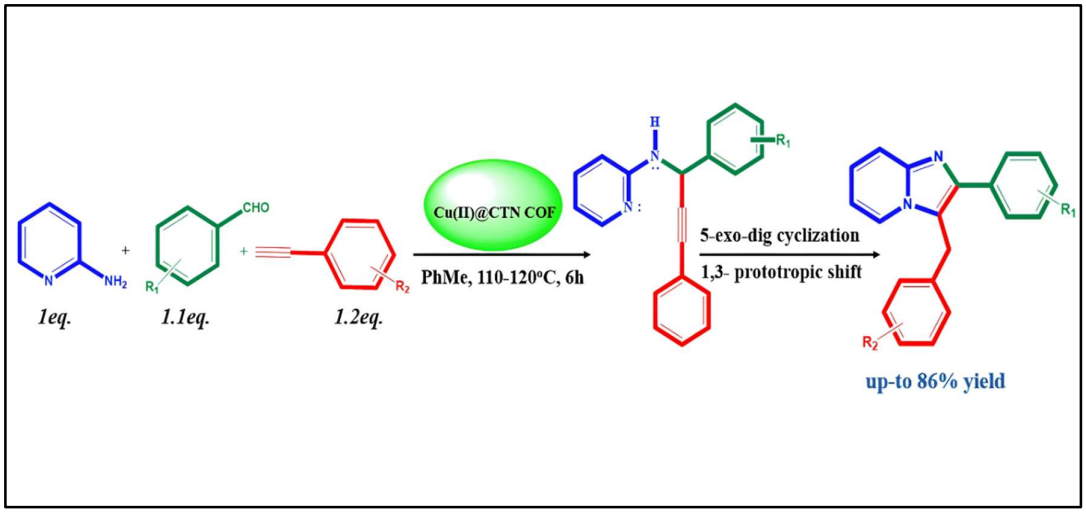

Scheme 5: Cascade Reaction Pathway Featuring A3-Coupling, Cyclization, and Prototropic Shift for the Synthesis of Imidazopyridines

Table 1: Optimization of reaction conditions with different Solvents and Catalysts

S.N	Catalyst	Solvent	Temperature (°C)	Time	Yield(%)[a]
1	No Catalyst	Ethanol	80	12h	0
2	$CuSO_4.5H_2O$	Ethanol	80	12h	49
3	$Cu(OAc)_2.H_2O$	Ethanol Toluene	80	12h 12h	58 61
4	CTN COF	Ethanol	80	12h	Trace
5	Cu(II)@ CTN COF	Acetonitrile	80	12h	52
6	Cu(II)@ CTN COF	Methanol	80	12h	62
7	Cu(II)@ CTN COF	THF	80	12h	44
8	Cu(II)@ CTN COF	DMF	110	10-12h	48
9	**Cu(II)@ CTN COF**	**Toluene**	**110**	**6-7h**	**79**

Reaction conditions: Catalyst (20mg), 2-aminopyridine (0.5 mmol), m-nitrobenzaldehyde (0.55 mmol), phenylacetylene (0.60 mmol). **a :** Isolated yield

Table 2: Dose optimization of catalyst

S.N	Amount of Catalyst	Time(h)	Yield(%)[a]
1	10	8h	60
2	15	8h	62
3	**20**	**6h**	**79**
4	25	6h	79

Reaction conditions: Catalyst (20mg), 2-aminopyridine (0.5 mmol), m-nitrobenzaldehyde (0.55 mmol), phenylacetylene (0.60 mmol). a: Isolated yield

To identify the most effective reaction conditions, a series of catalysts and solvents were screened, as summarized in **Table 1.** The reaction failed to proceed in the absence of a catalyst, and only modest yields were achieved with commonly used copper salts. Notably, the use of the Cu(II)@CTN COF catalyst resulted in a significant improvement in efficiency. Among the solvents evaluated, toluene delivered the highest yield when the reaction was carried out at 110 °C for 6 hours, affording the desired product in 79% yield. These findings highlight the importance of optimizing both the catalyst and the solvent to achieve maximum reaction efficiency. Similarly, Catalyst dosage was optimized **Table 2** by varying the amount of Cu(II)@CTN COF (Table 2). The best result was obtained with 20 mg of catalyst, yielding 79% product in 6 hours, while increasing the amount further showed no improvement. This confirms 20 mg as the optimal catalyst required for the efficient conversion.

Table 3: Synthesis of various derivatives of imidazo[1,2-a]pyridine

S.N	Derivative	Yield(%)[a]	Time	Melting point
1	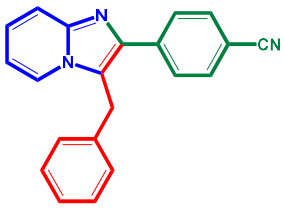	74	6.5h	134°C
2	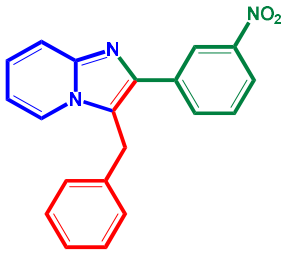	79	6h	136°C

3	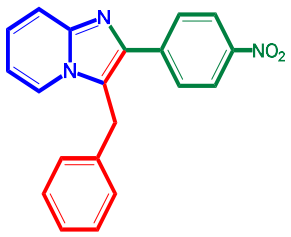	85	6h	164°C
4	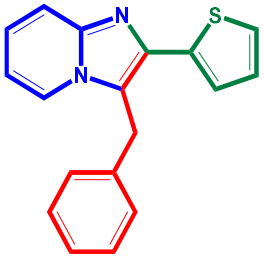	72	7h	154°C
5	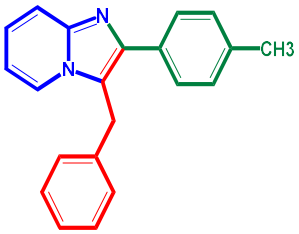	76	7.5h	207°C
6	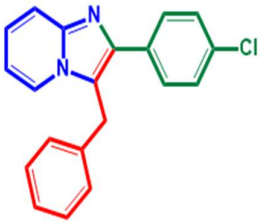	82	6h	148°C

7	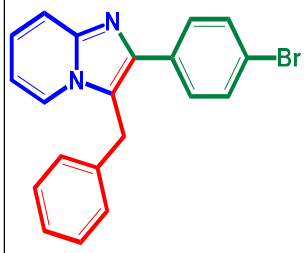	84	6h	160°C
8	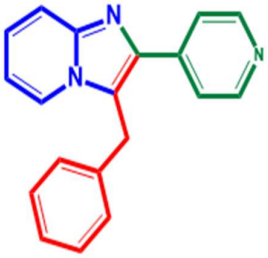	76	6.5h	124°C

Reaction conditions: Catalyst (20mg), 2-aminopyridine (0.5 mmol), m-nitrobenzaldehyde (0.55 mmol), phenylacetylene (0.60 mmol). **a: Isolated yield**

3.3 Plausible mechanism of the reaction

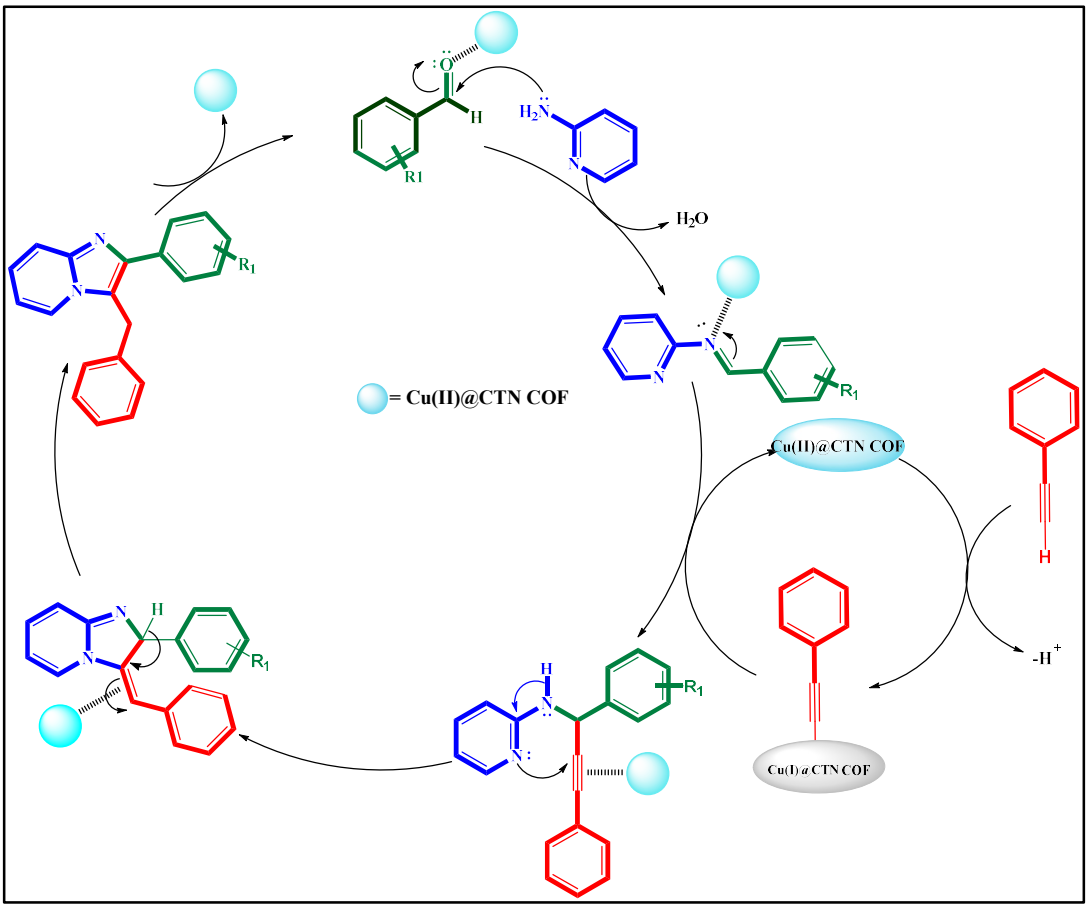

3.4 Experimental Section

3.4.1 Materials and Equipment

All chemicals, including aldehydes, 2-amino pyridine, and Phenylacetylene, were sourced commercially and used in the synthesis without further purification. The reaction took place in a pressure tube and was continuously tracked using Thin Layer Chromatography (TLC). Screening procedures were conducted using ethanol, methanol, DMF, THF, and Acetonitrile as solvents. Product purification was achieved through column chromatography with silica gel as the stationary phase. The analytical and spectral data for the synthesized compounds are included in the supplementary materials. IR spectra were recorded using an FT-IR spectrometer with KBr pellets, and NMR spectra were obtained using DMSO-d_6 and $CDCl_3$ as solvents. Melting points were determined using standard

melting point apparatus. All analytical and spectral characterization data of the synthesized compounds have been documented.

3.4.2 General synthetic procedure for the one-pot synthesis of imidazo[1,2-a]pyridine derivatives.

In a typical reaction, 2-aminopyridine 1.2 eq. (0.5 mmol), an aromatic aldehyde 1.1 eq. (0.55 mmol), and phenylacetylene1 eq. (0.5 mmol) were combined in toluene (suitable volume to maintain stirring) in the presence of Cu(II)@CTN COF catalyst (20 mg). The reaction mixture was stirred at 120 °C for 6 hours under atmospheric conditions. The progress of the reaction was monitored by thin-layer chromatography (TLC). Upon completion, the reaction mixture was cooled to room temperature and extracted with ethyl acetate. The combined organic layers were washed with brine and dried over anhydrous sodium sulphate(Na_2SO_4). After filtration and solvent evaporation under reduced pressure, the crude product was adsorbed onto neutral silica and purified by column chromatography using a mixture of ethyl acetate and hexane as the eluent to afford the desired imidazo[1,2-a]pyridine derivative.

3.4.3 Spectral data of 4-(3-benzylimidazo[1,2-a]pyridin-2-yl)benzonitrile

Off-White solid, m.p 134ºC, 74% Yield, IR v_{max}: 3043, 2223, 1676, 1610, 1494, 1450, 1356, 1258 cm−1;

^{1}H NMR (400 MHz, CDCl3) δ = 7.90 (d, J = 6.7 Hz, 2H), 7.74 (d, J = 6.8 Hz, 1H), 7.71−7.68 (m, 3H), 7.35−7.28 (m, 3H), 7.24− 7.21 (m, 1H), 7.12 (d, J = 6.8 Hz, 2H), 6.77 (dt, J = 6.8 Hz, J = 1.0 Hz, 1H), 4.51 (s, 2H);

^{13}C NMR (100 MHz, CDCl3) δ = 145.2, 142.0, 139.1, 136.0, 132.5, 129.2, 128.5, 127.6, 127.2, 125.1, 123.5, 119.0, 117.8, 112.8, 111.1, 29.8

3.4.4 Spectral data of 3-benzyl-2-(3-nitrophenyl)imidazo[1,2-a]pyridine

Yellow solid, m.p. 136 °C, IR: 3055, 2946, 2850, 1630, 1540, 1490, 1350.

^{1}H-NMR (CDCl3): 4.52 (s,CH2); 6.78 (t, J¼6.7, 1 H); 7.12 (d, J¼6.8, 2H); 7.22 (s, 1H); 7.25–7.40 (m, 3H); 7.72 (d, J¼8.9, 1H); 7.78 (d, J¼ 6.8, 1H); 7.98 (d, J¼8.9, 2H); 8.26 (d, J¼8.9, 2H).

^{13}C-NMR (CDCl3): 29.9; 112.8; 118.1; 119.5; 123.6; 124.2; 125.4; 127.5; 127.8; 128.6; 128.8; 136.2; 139.8; 141.8; 145.3; 147.2.

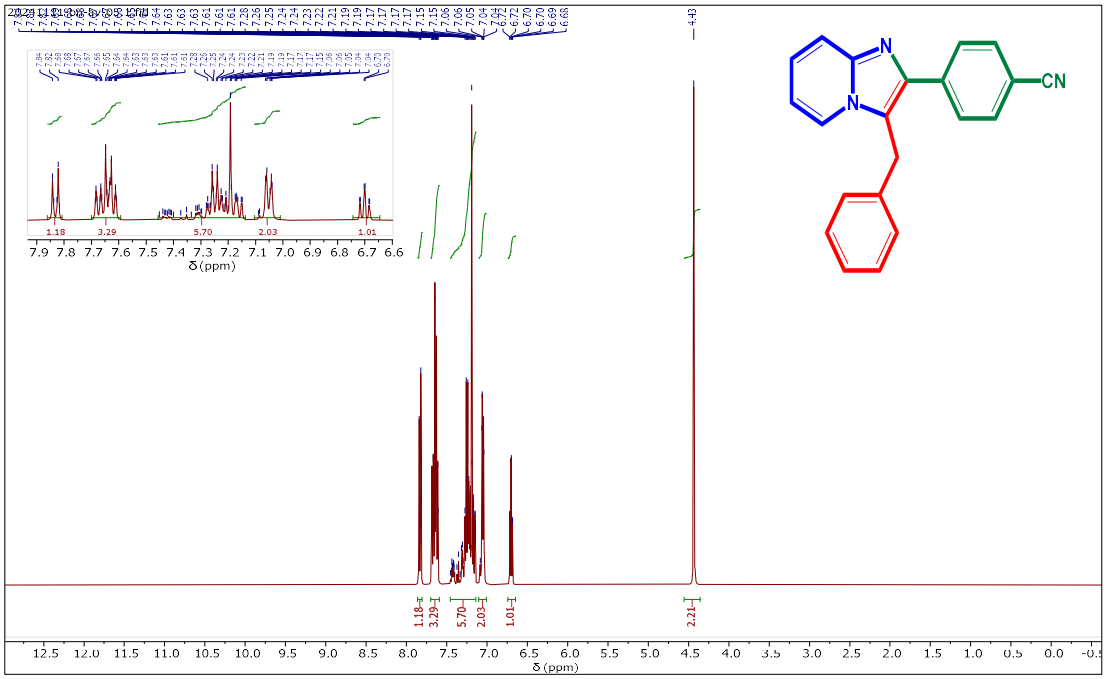

Spectra 1: ^{1}H NMR of 4-(3-benzylimidazo[1,2-a]pyridin-2-yl)benzonitrile

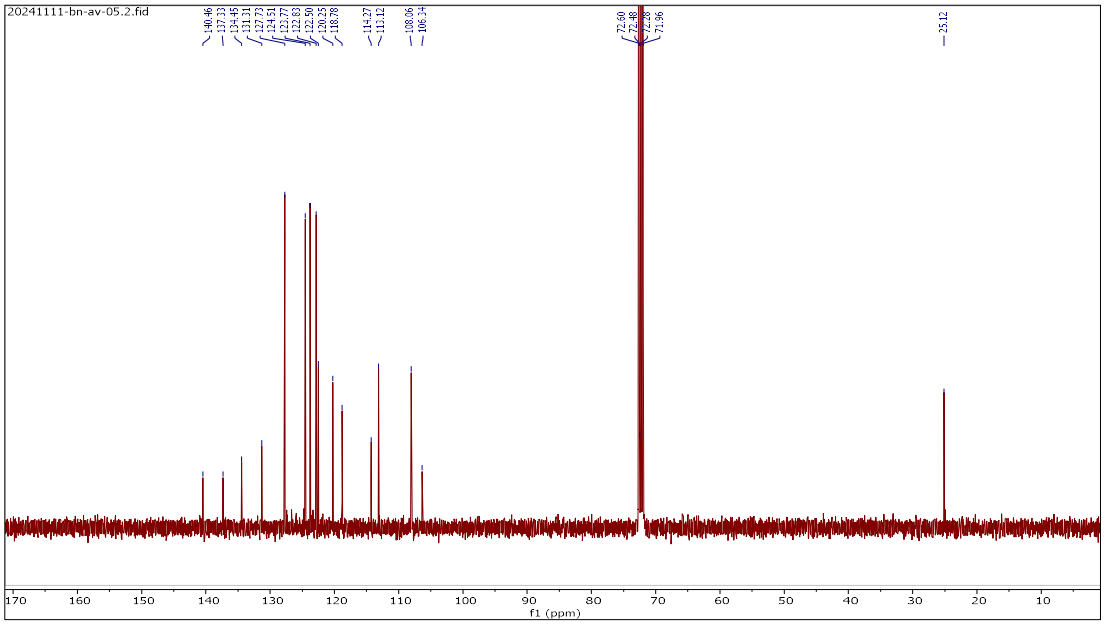

Spectra 2: ^{13}C NMR of 4-(3-benzylimidazo[1,2-a]pyridin-2-yl)benzonitrile

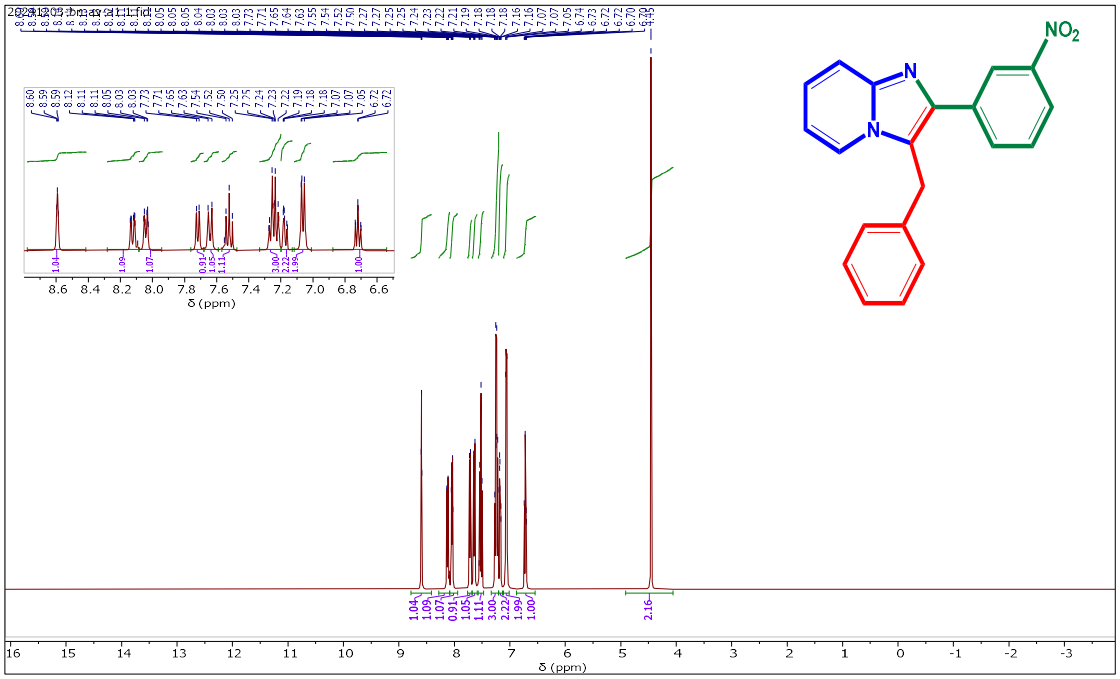

Spectra 3: 1H NMR of 3-benzyl-2-(3-nitrophenyl)imidazo[1,2-a]pyridine

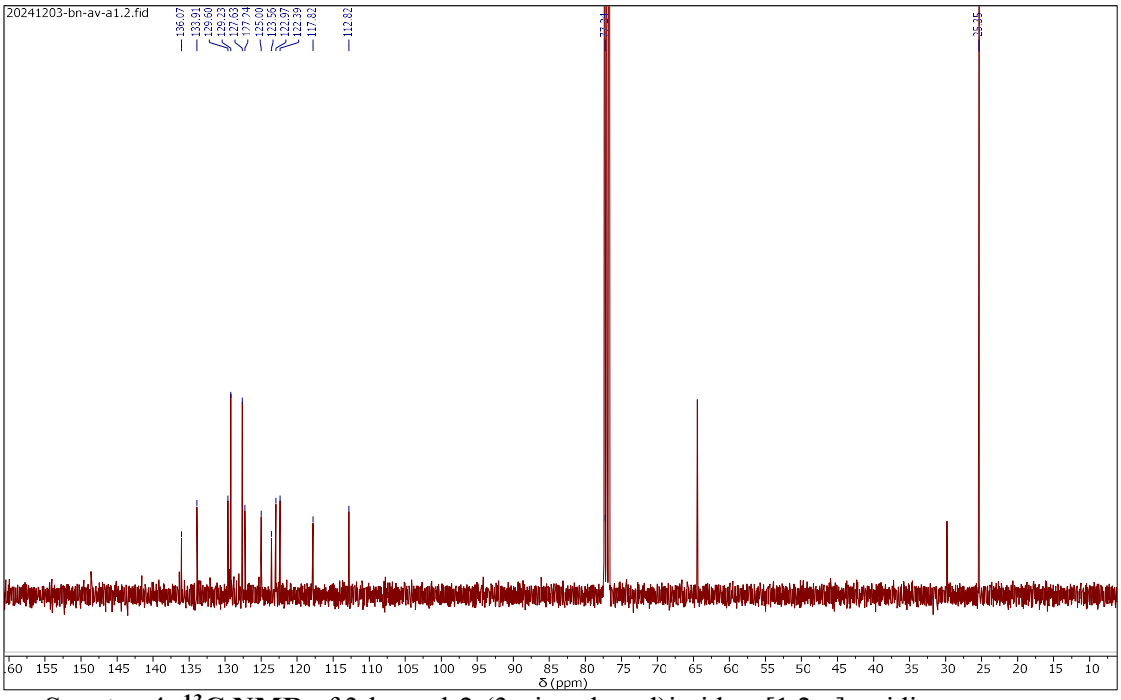

Spectra 4: ^{13}C NMR of 3-benzyl-2-(3-nitrophenyl)imidazo[1,2-a]pyridine

3.5 Recyclability of Cu(II)@CTN COF

The recyclability of the Cu(II)@CTN COF catalyst was evaluated through FT-IR spectroscopy over three consecutive catalytic cycles during the synthesis of imidazo[1,2-a]pyridine derivatives. The FT-IR spectra **(Figure 26)** display a comparative analysis of the catalyst before use and after each reaction cycle. The spectrum of the fresh Cu(II)@CTN COF (black trace) exhibits well-defined vibrational bands characteristic of the framework, including stretching vibrations in the regions around 1600 cm^{-1} and 1500 cm^{-1}, corresponding to C=N and aromatic C=C bonds, respectively. These peaks are preserved across the 1st (green), 2nd (purple), and 3rd (red) cycles, suggesting that the fundamental structure of the COF remains intact throughout repeated use.

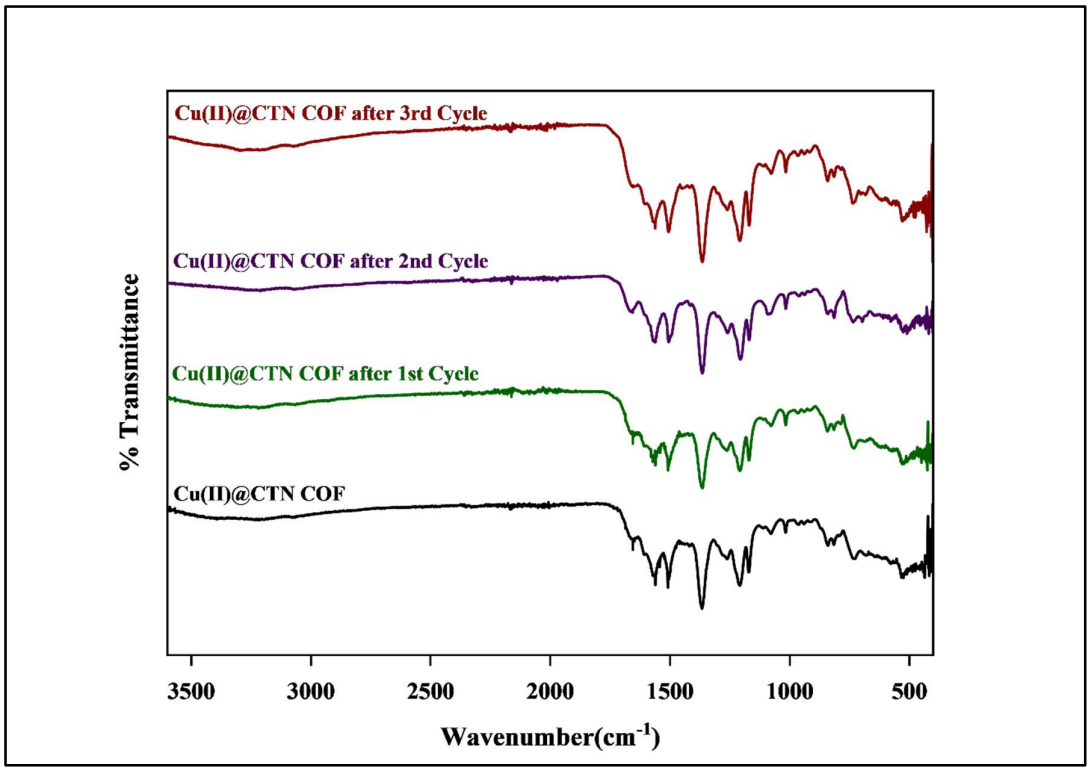

Fig. 26 Comparative FT-IR of fresh and used Catalyst

Although minor shifts and slight changes in intensity are observed in some bands after each cycle, particularly in the fingerprint region (1500–500 cm^{-1}), these variations are relatively modest. Such changes may be attributed to subtle interactions between the catalyst and the reaction media or to surface-bound intermediates. Importantly, the absence of significant spectral degradation or the emergence of new bands indicates that no major chemical decomposition or structural collapse occurs during recycling. This stability

highlights the robustness of the Cu(II)@CTN COF under the applied reaction conditions and confirms its potential as a reusable heterogeneous catalyst for imidazopyridine synthesis.

3.6 Conclusion

In this research, a covalent organic framework (CTN COF) was developed through a solvothermal synthesis route employing BTH and TTTB as the primary organic building blocks. Post-synthetic metalation with Cu(II) ions was carried out to generate the functionalized Cu(II)@CTN COF material. This catalyst was thoroughly characterized using a combination of analytical tools, including powder X-ray diffraction (P-XRD), BET surface area analysis, thermogravimetric analysis (TGA), X-ray photoelectron spectroscopy (XPS), Fourier-transform infrared spectroscopy (FT-IR), and field emission scanning electron microscopy (FE-SEM).

The resulting Cu(II)@CTN COF demonstrated notable catalytic performance in a one-pot cascade A^3-coupling followed by cyclization and prototropic shift, efficiently producing imidazo[1,2-a]pyridine derivatives. The methodology offered excellent yields (up to 86%) under relatively mild reaction conditions (PhMe, 110–120^{o}C, 6h). Additional benefits of this approach include a wide substrate compatibility, use of low-cost and easily accessible reactants, and strong reusability of the catalyst. Recyclability was confirmed through comparative FT-IR analysis over three catalytic cycles, where minimal change in characteristic peaks affirmed the catalyst's structural integrity and reusability. This work highlights the role of metal-loaded COFs as a versatile platform for precision-oriented organic transformations. Their structural tunability and stability make them highly suitable for advanced catalytic applications, underscoring their growing relevance in the field of green and sustainable chemistry.

References

[1] X. Ren *et al.*, "The Fabrication of Pd Single Atoms/Clusters on COF Layers as Co-catalysts for Photocatalytic H_2 Evolution," *ACS Appl Mater Interfaces*, vol. 14, no. 5, pp. 6885–6893, Feb. 2022, doi: 10.1021/acsami.1c23465.

[2] S. O. Akinnawo, "Covalent organic frameworks: Design, synthesis, characterization, and applications," Jan. 01, 2024, *Elsevier B.V.* doi: 10.1016/j.chphma.2023.08.003.

[3] Y. N. Gong, X. Guan, and H. L. Jiang, "Covalent organic frameworks for photocatalysis: Synthesis, structural features, fundamentals and performance," Jan. 15, 2023, *Elsevier B.V.* doi: 10.1016/j.ccr.2022.214889.

[4] S. Kandambeth, K. Dey, and R. Banerjee, "Covalent Organic Frameworks: Chemistry beyond the Structure," Feb. 06, 2019, *American Chemical Society*. doi: 10.1021/jacs.8b10334.

[5] A. P. Côté, A. I. Benin, N. W. Ockwig, M. O'Keeffe, A. J. Matzger, and O. M. Yaghi, "Porous, Crystalline, Covalent Organic Frameworks," *Science (1979)*, vol. 310, no. 5751, pp. 1166–1170, Nov. 2005, doi: 10.1126/science.1120411.

[6] S. S. Han, H. Furukawa, O. M. Yaghi, and W. A. Goddard, "Covalent Organic Frameworks as Exceptional Hydrogen Storage Materials," *J Am Chem Soc*, vol. 130, no. 35, pp. 11580–11581, Sep. 2008, doi: 10.1021/ja803247y.

[7] F. J. Uribe-Romo, J. R. Hunt, H. Furukawa, C. Klöck, M. O'Keeffe, and O. M. Yaghi, "A Crystalline Imine-Linked 3-D Porous Covalent Organic Framework," *J Am Chem Soc*, vol. 131, no. 13, pp. 4570–4571, Apr. 2009, doi: 10.1021/ja8096256.

[8] E. Jin *et al.*, "Two-dimensional sp^2 carbon–conjugated covalent organic frameworks," *Science (1979)*, vol. 357, no. 6352, pp. 673–676, Aug. 2017, doi: 10.1126/science.aan0202.

[9] Q. Fang *et al.*, "3D Porous Crystalline Polyimide Covalent Organic Frameworks for Drug Delivery," *J Am Chem Soc*, vol. 137, no. 26, pp. 8352–8355, Jul. 2015, doi: 10.1021/jacs.5b04147.

[10] S. Daliran, A. R. Oveisi, A. Dhakshinamoorthy, and H. Garcia, "Probing Defects in Covalent Organic Frameworks," *ACS Appl Mater Interfaces*, vol. 16, no. 38, pp. 50096–50114, Sep. 2024, doi: 10.1021/acsami.4c12069.

[11] S. Minami, M. Kin, K. Takahashi, T. Sato, and R. Jinnouchi, "Impact of Local Water Uptake on Proton Conduction in Covalent Organic Framework Revealed by Machine-Learning Potentials," *Chemistry of Materials*, vol. 36, no. 19, pp. 9535–9546, Oct. 2024, doi: 10.1021/acs.chemmater.4c01351.

[12] M.-X. Wu and Y.-W. Yang, “Applications of covalent organic frameworks (COFs): From gas storage and separation to drug delivery,” *Chinese Chemical Letters*, vol. 28, no. 6, pp. 1135–1143, Jun. 2017, doi: 10.1016/j.cclet.2017.03.026.

[13] X. Guan, F. Chen, Q. Fang, and S. Qiu, “Design and applications of three dimensional covalent organic frameworks,” *Chem Soc Rev*, vol. 49, no. 5, pp. 1357–1384, 2020, doi: 10.1039/C9CS00911F.

[14] L. Deng, Z. Ding, X. Ye, and D. Jiang, “Covalent Organic Frameworks: Chemistry of Pore Interface and Wall Surface Perturbation and Impact on Functions,” *Acc Mater Res*, vol. 3, no. 8, pp. 879–893, Aug. 2022, doi: 10.1021/accountsmr.2c00108.

[15] F. Haase and B. V. Lotsch, “Solving the COF trilemma: towards crystalline, stable and functional covalent organic frameworks,” *Chem Soc Rev*, vol. 49, no. 23, pp. 8469–8500, 2020, doi: 10.1039/D0CS01027H.

[16] Y. Li, W. Chen, G. Xing, D. Jiang, and L. Chen, “New synthetic strategies toward covalent organic frameworks,” *Chem Soc Rev*, vol. 49, no. 10, pp. 2852–2868, 2020, doi: 10.1039/D0CS00199F.

[17] H. M. El-Kaderi *et al.*, “Designed Synthesis of 3D Covalent Organic Frameworks,” *Science (1979)*, vol. 316, no. 5822, pp. 268–272, Apr. 2007, doi: 10.1126/science.1139915.

[18] R. K. Sharma *et al.*, “Recent development of covalent organic frameworks (COFs): Synthesis and catalytic (organic-electro-photo) applications,” Feb. 01, 2020, *Royal Society of Chemistry*. doi: 10.1039/c9mh00856j.

[19] Q. Qing *et al.*, “General synthesis of covalent organic frameworks under ambient condition within minutes via microplasma electrochemistry approach,” *Nature Communications* , vol. 16, no. 1, Dec. 2025, doi: 10.1038/s41467-025-57892-6.

[20] E. A. Gendy *et al.*, “Removal of heavy metals by covalent organic frameworks (COFs): A review on its mechanism and adsorption properties,” Aug. 01, 2021, *Elsevier Ltd*. doi: 10.1016/j.jece.2021.105687.

[21] L. Deng, Z. Ding, X. Ye, and D. Jiang, “Covalent Organic Frameworks: Chemistry of Pore Interface and Wall Surface Perturbation and Impact on Functions,” *Acc Mater Res*, vol. 3, no. 8, pp. 879–893, Aug. 2022, doi: 10.1021/accountsmr.2c00108.

[22] L. K. Ritchie, A. Trewin, A. Reguera-Galan, T. Hasell, and A. I. Cooper, “Synthesis of COF-5 using microwave irradiation and conventional solvothermal routes,” *Microporous and Mesoporous Materials*, vol. 132, no. 1–2, pp. 132–136, Jul. 2010, doi: 10.1016/j.micromeso.2010.02.010.

[23] Z. Alsudairy *et al.*, “Facile Microwave-Assisted Synthesis of 2D Imine-Linked Covalent Organic Frameworks for Exceptional Iodine Capture,” *Precision Chemistry*, vol. 1, no. 4, pp. 233–240, Jun. 2023, doi: 10.1021/prechem.3c00006.

[24] N. Brown *et al.*, “Green mechanochemical synthesis of imine-linked covalent organic frameworks for high iodine capture,” *Green Chemistry*, vol. 25, no. 16, pp. 6287–6296, 2023, doi: 10.1039/D3GC01927F.

[25] X. Wei, M. Bi, Q. Lou, D.-L. Di, B. Liu, and D. Pei, “Fast and Facile Sonochemical Fabrication of Covalent Organic Frameworks in Water for the Adsorption of Flavonoids: Adsorption Behaviors and Mechanisms,” 2024. doi: 10.2139/ssrn.4850923.

[26] J. L. Segura, S. Royuela, and M. Mar Ramos, “Post-synthetic modification of covalent organic frameworks,” Jul. 21, 2019, *Royal Society of Chemistry*. doi: 10.1039/c8cs00978c.

[27] M. Liu *et al.*, “Post-synthetic modification of covalent organic frameworks for CO2 electroreduction,” *Nat Commun*, vol. 14, no. 1, p. 3800, Jun. 2023, doi: 10.1038/s41467-023-39544-9.

[28] N. A. Rejali, M. Dinari, and Y. Wang, “Post-synthetic modifications of covalent organic frameworks (COFs) for diverse applications,” *Chemical Communications*, vol. 59, no. 78, pp. 11631–11647, 2023, doi: 10.1039/D3CC03091A.

[29] S.-Y. Ding *et al.*, “Construction of Covalent Organic Framework for Catalysis: Pd/COF-LZU1 in Suzuki–Miyaura Coupling Reaction,” *J Am Chem Soc*, vol. 133, no. 49, pp. 19816–19822, Dec. 2011, doi: 10.1021/ja206846p.

[30] J. Liu, N. Wang, and L. Ma, “Recent Advances in Covalent Organic Frameworks for Catalysis,” Feb. 03, 2020, *John Wiley and Sons Ltd*. doi: 10.1002/asia.201901527.

[31] J.-Y. Yue *et al.*, “Pd(II) functionalized vinylene-linked covalent organic frameworks for acidic electrocatalytic hydrogen evolution reaction,” *Microporous and Mesoporous Materials*, vol. 344, p. 112169, Oct. 2022, doi: 10.1016/j.micromeso.2022.112169.

[32] X. Li *et al.*, “Facile transformation of imine covalent organic frameworks into ultrastable crystalline porous aromatic frameworks,” *Nat Commun*, vol. 9, no. 1, p. 2998, Jul. 2018, doi: 10.1038/s41467-018-05462-4.

[33] H. Li, A. Dilipkumar, S. Abubakar, and D. Zhao, “Covalent organic frameworks for CO $_2$ capture: from laboratory curiosity to industry implementation,” *Chem Soc Rev*, vol. 52, no. 18, pp. 6294–6329, 2023, doi: 10.1039/D2CS00465H.

[34] S. Wei *et al.*, “Functionalized 3D Covalent Organic Frameworks for High-Performance CO $_2$ Capture and Separation over N $_2$,” *Adv Theory Simul*, vol. 5, no. 12, Dec. 2022, doi: 10.1002/adts.202200588.

[35] G. B. Wang *et al.*, “Covalent organic frameworks: emerging high-performance platforms for efficient photocatalytic applications,” *J Mater Chem A Mater*, vol. 8, no. 15, pp. 6957–6983, Apr. 2020, doi: 10.1039/d0ta00556h.

[36] S. S. A. Shah *et al.*, “Covalent Organic Frameworks (COFs) for heterogeneous catalysis: Recent trends in design and synthesis with structure-activity relationship,” *Materials Today*, vol. 67, pp. 229–255, Jul. 2023, doi: 10.1016/j.mattod.2023.05.023.

[37] G. J. Chen *et al.*, “Ru Nanoparticles-Loaded Covalent Organic Framework for Solvent-Free One-Pot Tandem Reactions in Air,” *Inorg Chem*, vol. 57, no. 5, pp. 2678–2685, Mar. 2018, doi: 10.1021/acs.inorgchem.7b03077.

[38] J. Li *et al.*, “Metal-free covalent organic frameworks containing precise heteroatoms for electrocatalytic oxygen reduction reaction,” *J Mater Chem A Mater*, vol. 11, no. 34, pp. 18349–18355, 2023, doi: 10.1039/D3TA03534D.

[39] K. Zhang *et al.*, “Raising the Asymmetric Catalytic Efficiency of Chiral Covalent Organic Frameworks by Tuning the Pore Environment,” *ACS Appl Mater Interfaces*, vol. 16, no. 8, pp. 10661–10670, Feb. 2024, doi: 10.1021/acsami.3c17048.

[40] Y. Wang *et al.*, “Blue light photocatalytic oxidation of sulfides to sulfoxides with oxygen over a thiazole-linked 2D covalent organic framework,” *Appl Catal B*, vol. 338, p. 123070, Dec. 2023, doi: 10.1016/j.apcatb.2023.123070.

[41] M. Cui *et al.*, “Covalent organic framework with Cu-containing compounds for enhancing flame retardancy and smoke suppression effects on epoxy resin,” *Compos Part A Appl Sci Manuf*, vol. 156, May 2022, doi: 10.1016/j.compositesa.2022.106900.

[42] S. Bhagat, S. Wahurwagh, A. Verma, and U. Pratap, “Harnessing synergy: Immobilized Cu(II) and Pd(II) species on magnetic silica-coated copper ferrite for A3 and Sonogashira coupling reactions,” *Appl Surf Sci*, vol. 687, Apr. 2025, doi: 10.1016/j.apsusc.2024.162264.

[43] D. Chakraborty, S. Nandi, D. Mullangi, S. Haldar, C. P. Vinod, and R. Vaidhyanathan, “Cu/Cu 2 O Nanoparticles Supported on a Phenol-Pyridyl COF as a Heterogeneous Catalyst for the Synthesis of Unsymmetrical Diynes via Glaser-Hay Coupling,” *ACS Appl Mater Interfaces*, vol. 11, no. 17, pp. 15670–15679, May 2019, doi: 10.1021/acsami.9b02860.

[44] *, †NicolasBlanchard, *, ‡andMathieuToumi† GwilhermEvano, “opper-MediatedCouplingReactionsandTheirApplicationsinNatural ProductsandDesigne dBiomoleculesSynthesis,” *Chem.Rev.2008,108,3054–3131*.

[45] C. Enguehard-Gueiffier and A. Gueiffier, “Recent Progress in the Pharmacology of Imidazo[1,2-a]pyridines,” *Mini-Reviews in Medicinal Chemistry*, vol. 7, no. 9, pp. 888–899, Sep. 2007, doi: 10.2174/138955707781662645.

[46] S. M. Hanson, E. V. Morlock, K. A. Satyshur, and C. Czajkowski, “Structural Requirements for Eszopiclone and Zolpidem Binding to the γ-Aminobutyric Acid Type-A (GABA $_A$) Receptor Are Different,” *J Med Chem*, vol. 51, no. 22, pp. 7243–7252, Nov. 2008, doi: 10.1021/jm800889m.

[47] M. F. L. R. A. L. G. G. E. S. F. T. E. C. G. B. G. L. G Trapani 1, "Synthesis and binding affinity of 2-phenylimidazo[1,2-alpha]pyridine derivatives for both central and peripheral benzodiazepine receptors. A new series of high-affinity and selective ligands for the peripheral type." doi: 10.1021/jm970112.

[48] A. K. T. M. G. K. I. T. K. Y. M. Y. Maruyama Y, "Anti-inflammatory activity of an imidazopyridine derivative (miroprofen). Arzneimittelforschung," *Arzneimittelforschung*.

[49] J. G. Lombardino, "Chapter 18. New Agents for the Treatment of Inflammation and Arthritis," 1981, pp. 189–198. doi: 10.1016/S0065-7743(08)61285-3.

[50] J. R. Henry *et al.*, "6-Amino-2-(4-fluorophenyl)-4-methoxy-3- (4-pyridyl)-1 *H* -pyrrolo[2,3- *b*]pyridine (RWJ 68354): A Potent and Selective p38 Kinase Inhibitor," *J Med Chem*, vol. 41, no. 22, pp. 4196–4198, Oct. 1998, doi: 10.1021/jm980497b.

[51] C. Martini, M. I. D. Mardjan, and A. Basso, "The Groebke–Blackburn–Bienaymé reaction in its maturity: innovation and improvements since its 21st birthday (2019–2023)," 2024, *Beilstein-Institut Zur Forderung der Chemischen Wissenschaften*. doi: 10.3762/bjoc.20.162.

[52] Y. Volkova, S. Baranin, and I. Zavarzin, "A3 Coupling Reaction in the Synthesis of Heterocyclic Compounds," Jan. 05, 2021, *Wiley-VCH Verlag*. doi: 10.1002/adsc.202000866.

[53] P. Puthiaraj, A. Ramu, and K. Pitchumani, "Copper-based metal-organic frameworks as reusable heterogeneous catalysts for the one-pot syntheses of imidazo[1,2-a]pyridines," *Asian J Org Chem*, vol. 3, no. 7, pp. 784–791, 2014, doi: 10.1002/ajoc.201402019.

[54] A. Maleki, "Synthesis of Imidazo[1,2-a]pyridines Using Fe 3 O 4 @SiO 2 as an Efficient Nanomagnetic Catalyst via a One-Pot Multicomponent Reaction."

[55] A. Dömling, W. Wang, and K. Wang, "Chemistry and biology of multicomponent reactions," Jun. 13, 2012. doi: 10.1021/cr100233r.

[56] A. Dömling, "Recent developments in isocyanide based multicomponent reactions in applied chemistry," Jan. 2006. doi: 10.1021/cr0505728.

[57] I. Kim *et al.*, "Design, synthesis, and evaluation of 2-aryl-7-(3′,4′-dialkoxyphenyl)-pyrazolo[1,5-a]pyrimidines as novel PDE-4 inhibitors," *Bioorg Med Chem Lett*, vol. 20, no. 3, pp. 922–926, Feb. 2010, doi: 10.1016/j.bmcl.2009.12.070.

[58] R. Mariai *et al.*, "Bridging Pharmaceutical Chemistry with Drug and Nanoparticle Targeting to Investigate the Role of the 18-kDa TranslocatorProtein TSPO", doi: 10.1002/cmdc.v12.16/issuetoc.

[59] N. Chernyak and V. Gevorgyan, "General and Efficient Copper-Catalyzed Three-Component Coupling Reaction towards Imidazoheterocycles: One-Pot Synthesis

of Alpidem and Zolpidem," *Angewandte Chemie International Edition*, vol. 49, no. 15, pp. 2743–2746, Apr. 2010, doi: 10.1002/anie.200907291.

[60] J. S. Yadav, B. V. S. Reddy, and Y. J. Reddy, "A rapid synthesis of 3-sulfenyl indoles using Selectfluor™," *Tetrahedron Lett*, vol. 48, no. 39, pp. 7034–7037, Sep. 2007, doi: 10.1016/j.tetlet.2007.07.130.

[61] S. Mishra and R. Ghosh, "Mechanistic Studies on a New Catalyst System (CuI-NaHSO4×SiO2) Leading to the One-Pot Synthesis of Imidazo[1,2-a]pyridines from Reactions of 2-Aminopyridines, Aldehydes, and Terminal Alkynes," *Synthesis (Stuttg)*, vol. 2011, no. 21, pp. 3463–3470, Nov. 2011, doi: 10.1055/s-0030-1260255.

[62] S. K. Guchhait, A. L. Chandgude, and G. Priyadarshani, "$CuSO_4$ –Glucose for in Situ Generation of Controlled Cu(I)–Cu(II) Bicatalysts: Multicomponent Reaction of Heterocyclic Azine and Aldehyde with Alkyne, and Cycloisomerization toward Synthesis of N-Fused Imidazoles," *J Org Chem*, vol. 77, no. 9, pp. 4438–4444, May 2012, doi: 10.1021/jo3003024.